

Supporting Information

Directed Evolution of Cyclic Peptides for Inhibition of Autophagy

Joshua P. Gray¹, Md. Nasir Uddin¹, Rajan Chaudhari², Margie N. Sutton¹, Hailing Yang², Philip Rask², Hannah Locke³, Brian J. Engel¹, Nefeli Batistatou⁴, Jing Wang⁴, Brian J. Grindel¹, Pratip Bhattacharya¹, Seth T. Gammon¹, Shuxing Zhang², David Piwnica-Worms¹, Joshua A. Kritzer⁴, Zhen Lu², Robert C. Bast Jr.², Steven W. Millward^{1*}.

1. Department of Cancer Systems Imaging, University of Texas MD Anderson Cancer Center
2. Department of Experimental Therapeutics, University of Texas MD Anderson Cancer Center
3. Department of Biology and Biochemistry, University of Houston
4. Department of Chemistry, Tufts University

*To whom correspondence should be addressed (smillward@mdanderson.org)

Table of Contents

Supplemental Methods.....	4
Table S1: Statistical Parameters from Figures 6 and 7.....	10
Figure S1: SDS-PAGE and Autoradiography and <i>in vitro</i> translated Atg8 homologs.....	11
Figure S2: Sequence Alignment of LC3 Homologs.....	12
Figure S3: Binding of SUPR4B1W and scrambled SUPR4B1W to LC3A and LC3B by FP.....	13
Figure S4: Representative Images from GFP-LC3 Puncta Inhibition Experiment.....	14
Figure S5: Effect of Scrambled SUPR4B1W on OVCAR8 and Hey cell line viability.....	15
Figure S6: Effect of SUPR4B1W and cisplatin on cancer cell line viability.....	16
Figure S7: Effect of SUPR4B1W on Hey and OVCAR8 Cells	17
Figure S8: ESI-MS of NVOC-N-methylalanine-OCN and NVOC-N-methylalanine-pdCpA.....	18
Figure S9: ESI-MS and HPLC of SUPR4B (linear).....	19
Figure S10: ESI-MS and HPLC of SUPR4B-fluorescein (linear).....	20
Figure S11: ESI-MS and HPLC of SUPR4B (cyclic).....	21
Figure S12: ESI-MS and HPLC of SUPR4B-fluorescein (cyclic).....	22
Figure S13: ESI-MS and HPLC of SUPR4B1W (linear).....	23
Figure S14: ESI-MS and HPLC of SUPR4B1W-fluorescein (linear).....	24
Figure S15: ESI-MS and HPLC of SUPR4B1W (cyclic).....	25
Figure S16: ESI-MS and HPLC of SUPR4B1W-fluorescein (cyclic).....	26
Figure S17: ESI-MS and HPLC of SUPR4B1W-biotin (cyclic).....	27
Figure S18: ESI-MS and HPLC of SUPR4B1W8A (linear).....	28
Figure S19: ESI-MS and HPLC of SUPR4B1W8A-fluorescein (linear).....	29
Figure S20: ESI-MS and HPLC of SUPR4B1W8A (cyclic).....	30
Figure S21: ESI-MS and HPLC of SUPR4B1W8A-fluorescein (cyclic).....	31
Figure S22: ESI-MS and HPLC of SUPR4B1W-ROX (cyclic).....	32
Figure S23: ESI-MS and HPLC of SUPR4B1W scrambled.....	33

Figure S24: ESI-MS and HPLC of Chloroalkane azide.....	34
Figure S25: ESI-MS and HPLC of ct-SUPR4B1W.....	35
Figure S26: ESI-MS and HPLC of ct-SUPR4B1W scrambled.....	36
Figure S27: ESI-MS and HPLC of ct-SUPR4B1W linear.....	37
Figure S28: ESI-MS and HPLC of ct-SUPR4B1W8A.....	38
References.....	39

Supplemental Methods

Expression and Purification of Recombinant LC3

pQTEV-MAP1LC3A vectors for expression and purification of N-terminally polyhistidine tagged recombinant LC3A were ordered through Addgene (Plasmid #34824) and transformed into BL21-DE3 pLysS *E. coli* (Promega). 2 Liters of LB media were inoculated from overnight cultures and grown to an OD₆₀₀ of 0.6 before expression was induced with IPTG at a concentration of 0.6 mM for 3 hours. Cell pellets were resuspended in 15 mL equilibration buffer (20 mM HEPES pH 7.2, 200 mM NaCl, 10 mM imidazole) and lysed by sonication. Clarified lysate was incubated with 1 mL Ni-NTA resin for one hour, loaded onto a fritted column, and flow-through eluted. Resin was washed four times with equilibration buffer and the protein was eluted with 15 mL elution buffer (20 mM HEPES pH 7.2, 200 mM NaCl, 250 mM imidazole). Eluted protein was buffer exchanged against dialysis buffer (20 mM HEPES pH 7.2, 200 mM NaCl, 25% glycerol) using 3,000 MWCO dialysis tubing (Fisher) and concentrated by Amicon Ultracel 3k centrifugal filters (Millipore) to a final concentration of 1.4 mg/mL (7 mg/L total yield). His6-LC3A was biotinylated using 5x molar excess biotin-NHS (Sigma). The reaction was incubated on ice for 2 hours before excess biotin-NHS was removed by 7,000 MWCO Zeba spin column (Thermo). Biotinylation was confirmed by HABA-Avidin assay (Pierce) and the final concentration of biotinylated His6-LC3A was measured at 1.25 mg/mL by BCA assay.

pDEST15-LC3A and pDEST15-LC3B constructs for N-terminally tagged GST-LC3A and GST-LC3B were provided by Dr. Terje Johansen^{1,2}. Transformation and expression of plasmids were performed as described above. Clarified lysate was incubated with 1 mL glutathione agarose (Goldbio) for one hour, loaded onto a fritted column, and flow-through eluted. Resin was washed four times with equilibration buffer and the protein was eluted with 15 mL elution buffer (20 mM HEPES pH 7.2, 200 mM NaCl, 10 mM reduced glutathione). Eluted protein was exchanged against dialysis buffer (20 mM HEPES pH 7.2, 200 mM NaCl, 25% glycerol) using 3,000 MWCO dialysis tubing (Fisher) and concentrated by Amicon Ultracel 3k centrifugal filters (Millipore) to a final concentration of 1.18 mg/mL (11.8 mg yield per liter of culture) GST-LC3A and 1.13 mg/mL (11.3 mg yield per liter of culture) GST-LC3B by BCA assay.

Synthesis of N-methyl Alanine amber codon suppressor tRNA

NVOC-N-methyl-L-alanine cyanomethyl ester was synthesized according to previously described protocols for conjugation to the dinucleotide pdCpA and ligation to the amber suppressor THG73 tRNA³. NVOC-Cl (269 mg, 970 μmol, Sigma) was dissolved in 8 mL THF and added dropwise to N-methyl-L-alanine (100 mg, 969.7 μmol, Sigma) dissolved in 2 mL 100mM sodium carbonate. 10 N NaOH was added to bring the reaction mixture to pH > 10 and the reaction mixture was stirred at room temperature protected from light for 3 hours. Solvents were removed *in vacuo* and the dried compound was dissolved in 3 mL dry DMF to which 2 mL chloroacetonitrile and 600 μL triethylamine were added. The reaction was stirred under nitrogen overnight before the solvents were

removed *in vacuo* and the remaining solid was purified by silica gel flash chromatography with EtOAc/hexanes (3:1) yielding 84.6 mg NVOC-N-methyl-L-alanine cyanomethyl ester (22.8% yield) (**Figure S8A**).

NVOC-N-methyl-L-alanine cyanomethyl ester (12.7 mg, 33.2 μmol) and pdCpA (5 mg, 8.3 μmol , TriLink Biotechnologies) were dissolved in 400 μL dry DMF under nitrogen and stirred at room temperature protected from light for 4 hours before quenching the reaction with 20 μL ammonium acetate (25 mM, pH 4.5). The crude product was purified by reverse phase preparative HPLC using a gradient of ammonium acetate (25 mM, pH 4.5) to acetonitrile and the fractions corresponding to the product were combined and lyophilized yielding 3 mg of NVOC-N-Methyl-L-Alanine-pdCpA (36.1% yield). Product was confirmed by observing the $[M+H]^+$ peak at MW = 961.54 (expected 960.21) using electrospray ionization mass spectrometry (**Figure S8B**).

pUC19-THG73tRNA plasmid (a gift from Dennis Dougherty, California Institute of Technology) containing the gene for THG73 amber codon suppressor tRNA was PCR amplified and linearized by overnight FokI digestion at 37°C. THG73 tRNA was transcribed *in vitro* by T7 RNA polymerase, purified by Urea-PAGE and dissolved in water (2 $\mu\text{g}/\mu\text{L}$ final concentration).

NVOC-N-methyl-L-alanine-pdCpA was ligated to THG73 tRNA just prior to its use in *in vitro* translation reactions. THG73 tRNA (20 μg in 10 μL water) and HEPES (20 μL , 10 mM, pH 7.5) were combined and heated at 95 °C for 3 minutes, then cooled to 37 °C. NVOC-N-Methyl-L-Alanine-pdCpA (8 μL , 3 mM in DMSO) was added to the tRNA-HEPES mixture along with water (30 μL), T4 RNA Ligase (4 μL , New England Biolabs), and 10x T4 Reaction Buffer (8 μL , New England Biolabs). The reaction was incubated at 37 °C for 65 minutes, extracted with 25:24:1 phenol:chloroform:isoamyl alcohol (Sigma), and precipitated with >3 volumes cold ethanol at -80 °C. The precipitate was dried by vacuum, dissolved in 20 μL 1 mM sodium acetate, quantified by measuring A_{260} , and adjusted to a final concentration of 1 $\mu\text{g}/\mu\text{L}$. Immediately prior to *in vitro* translation the AA-tRNA solution was deprotected by short-wave UV for 15 minutes.

Sanger Sequencing

After library convergence, the final pool was TOPO-TA cloned into pCR™II-TOPO® vector (Thermo-Fisher), transformed into One Shot TOP10 chemically competent *E. coli* (Thermo-Fisher), and plated on ampicillin-agarose to isolate individual sequences from the final selection pool. Twelve colonies from each parallel selection were selected at random and plasmid minipreps (Life Technologies) were prepared from 5 mL overnight cultures. Amplified plasmids were submitted for Sanger sequencing at the MD Anderson Advanced Technology Genomics Core and analyzed using FinchTV software.

Peptide Synthesis and Cyclization

Peptides were synthesized using a Prelude automated peptide synthesis instrument (Protein Technology, Inc.). 2-chlorotrityl resin (0.439 g, 0.5 mmol, Advanced Chemtech) was swollen in DMF for 1 hour and washed twice with 5 mL DMF. The initial C-terminal amino acid coupling to the resin was performed manually prior to

automated synthesis of peptides. 2 equivalents Fmoc-propargylglycine (1 mmol, 335 mg) and 3 equivalents N,N-diisopropylethylamine (DIEA, 1.5 mmol, 262 μ L, Sigma) were added to the swelled resin in 6 mL DMF and rotated at room temperature for 1 hour. To synthesize each peptide, 100 mg of Fmoc-propargylglycine resin was loaded onto the automated synthesis instrument and synthesis was performed with 3 equivalents of Fmoc amino acid (Oakwood Products, Inc.), DIEA, and N,N,N',N'-Tetramethyl-O-(1H-benzotriazol-1-yl)uronium hexafluorophosphate (HBTU, Oakwood Products, Inc.) in N-methyl Pyrrolidone (NMP). A total of 3 coupling reactions (10 minute duration) were performed for each amino acid building block. Deprotection of Fmoc groups was achieved using 20% (v/v) piperidine in NMP. After synthesis and final deprotection, the resin was washed 5x with NMP (1.5 mL, 2.5 minutes), 5x with DCM (1.5 mL, 2.5 minutes), and dried under vacuum for 1 hour. Peptides were cleaved from the resin with 95% (v/v) trifluoroacetic acid, 2.5% (v/v) water, 2.5% (v/v) triisopropylsilane at room temperature for 3 hours, precipitated with cold diethyl ether, and dried under vacuum. Crude products were purified by reverse phase preparative HPLC (Luna Phenomenex, 5 μ m C18(2), 250 mm x 21.2 mm LC column) using gradient elution (5-95% Buffer B over 45 minutes; Buffer A dH₂O + 0.1% (v/v) TFA, Buffer B CH₃CN + 0.1% (v/v) TFA). Appropriate fractions were combined and lyophilized yielding a white solid. Purified products were confirmed by electrospray ionization mass spectrometry. HPLC chromatograms and mass spectra for each peptide may be found in the **Supplemental Figures S9, S13, and S18**.

Amine reactive cross-linker chemistry was utilized to cyclize peptides between the N-terminus of the peptide and the side-chain of a C-terminal lysine residue. Purified linear peptide was dissolved in DMF and mixed with 1.1 equivalents of disuccinimidyl glutarate (DSG) and 7 equivalents DIEA at room temperature for 3 hours. After 3 hours the reaction was quenched with hydroxylamine (10 mM final concentration) for 15 minutes and solvent was removed *in vacuo*. The crude product was dissolved in 1 mL 95:5 (v/v) dH₂O:CH₃CN + 0.1% (v/v) TFA and purified by reverse phase preparative HPLC using gradient elution (5-20% Buffer B over 5 minutes, 20-95% Buffer B over 60 minutes; Buffer A dH₂O + 0.1% (v/v) TFA, Buffer B CH₃CN + 0.1% (v/v) TFA). Appropriate fractions were combined and lyophilized yielding a white solid. Purified products were confirmed by electrospray ionization mass spectrometry. HPLC chromatograms and mass spectra for each peptide may be found in **Supplemental Figures S11, S15, S20, and S23**.

Fluorophore Conjugation of SUPR Peptides

Copper-catalyzed click chemistry was used to conjugate fluorescein-azide to the side-chain alkyne of the C-terminal propargylglycine residue in SUPR peptides. Between 2-3 μ mol of each peptide was dissolved in DMSO and added to 1.2 equivalents FAM-azide, 6-isomer (50 mg/mL, Lumiprobe), 50 μ L click solution (16 mg/mL CuSO₄·2H₂O and 30 mg/mL L-ascorbic acid in dH₂O), 5 μ L of tris-(benzyltriazolylmethyl)amine (TBTA, 100 mg/mL in DMF). Reaction mixture was brought to a final volume of 150 μ L with dH₂O and rotated at room temperature for 2 hours and purified by reverse phase preparative HPLC (Luna Phenomenex, 5 μ m C18(2), 250 mm x 21.2 mm LC column) using gradient elution (5-95% Buffer B over 45 minutes; Buffer A dH₂O + 0.1% (v/v) TFA, Buffer B CH₃CN + 0.1% (v/v) TFA). Appropriate fractions were combined and lyophilized yielding a yellow-

green solid. Purified products were confirmed by electrospray ionization mass spectrometry. HPLC chromatograms and mass spectra for each peptide may be found in the **Supplemental Figures S10, S12, S14, S16, S19, and S21**.

Fluorescence Polarization Assays

For fluorescence polarization assays, stock solutions of GST, GST-LC3A and GST-LC3B were adjusted to 5 μ M and serially diluted to concentrations between 5 μ M and 2.4 nM in triplicate in black polystyrene 96-well plates (Corning). FAM-labeled peptide was added to each well to a final concentration of 10 nM and incubated at room temperature for 2 hours. Fluorescence polarization was measured on a Biotek Synergy Neo Microplate Reader using a dual PMT FP 485/528 filter set. The mean value of polarization was calculated for each sample concentration and mean polarization values for GST were subtracted from GST-LC3 measurements to eliminate any effects from non-specific interactions. Mean fluorescence polarization measurements were converted to fluorescence anisotropy and fit to a one-site saturation binding model in Graphpad Prism 8 to calculate equilibrium binding constants for each peptide. The values shown in Table1 represent the mean value and the error bars represent the standard error.

Biotin Conjugation of SUPR

Copper-catalyzed click chemistry was used to conjugate biotin-azide to the side-chain alkyne of the C-terminal propargylglycine residue in SUPR peptides. 2 μ mol of SUPR4B1W was dissolved in DMSO and added to 1.2 equivalents Biotin-PEG3-azide (Thermo-Fisher), 50 μ L click solution (16 mg/mL CuSO₄·2H₂O and 30 mg/mL L-ascorbic acid in dH₂O), 5 μ L of tris-(benzyltriazolylmethyl)amine (TBTA, 100 mg/mL). The reaction mixture was brought to a final volume of 150 μ L with dH₂O and rotated at room temperature for 2 hours and purified by reverse phase preparative HPLC (Luna Phenomenex, 5 μ m C18(2), 250 mm x 21.2 mm LC column) using gradient elution (5-95% Buffer B over 45 minutes; Buffer A dH₂O + 0.1% (v/v) TFA, Buffer B CH₃CN + 0.1% (v/v) TFA). Appropriate fractions were combined and lyophilized yielding 2.8 mg of white solid (70.5% yield). Purified products were confirmed by electrospray ionization mass spectrometry. HPLC chromatograms and mass spectra are found in **Supplemental Figure S17**.

Fluorescence microscopy

HeLa cells stably expressing eGFP-LC3 were seeded at a density of 30,000 cells/well in an 8-well chambered coverslide (Corning) 24 hours before beginning treatment. Cells were treated with complete media supplemented with 500 nM SUPR4B1W-ROX for 12 hours. After 12 hours cells were either starved with Hank's Balanced Salt Solution (Corning) or were given fresh complete media for 2 hours and then subjected to live-cell fluorescence confocal imaging.

Quantification of colocalization between SUPR4B1W-ROX and eGFP-LC3 puncta was performed in ImageJ. Three fields of images for both starved and unstarved treatments were selected and split into red and

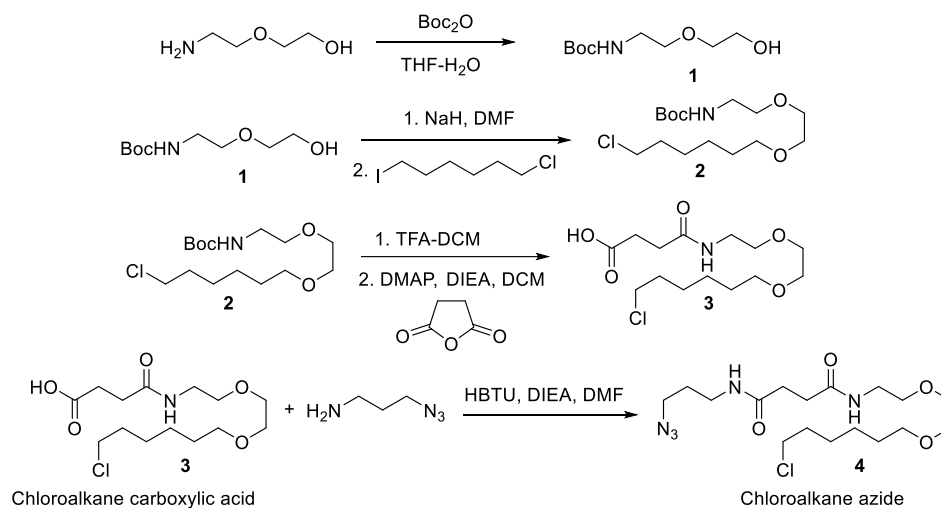
green channels. Cells that were mitotic or had lost eGFP-LC3 expression were removed from the analysis. Manders M1 and M2 coefficients were calculated using the Just Another Colocalization (JACoP)⁴ plugin using appropriate pixel intensity thresholding to filter background signal.

Synthesis of SUPR4B1W-ROX

Copper-catalyzed click chemistry was used to conjugate carboxy-X-rhodamine (ROX) azide to the side-chain alkyne of the C-terminal propargylglycine residue of SUPR4B1W. 3 μmol of SUPR4B1W was dissolved in DMSO and added to 1.2 eq ROX-azide (50 mg/mL, Lumiprobe), 50 μL click solution (16 mg/mL $\text{CuSO}_4 \cdot 2\text{H}_2\text{O}$ and 30 mg/mL L-ascorbic acid in dH_2O), 5 μL of TBTA (100 mg/mL). Reaction mixture was brought to a final volume of 150 μL with dH_2O and rotated at room temperature for 2 hours and purified by reverse phase preparative HPLC (Luna Phenomenex, 5 μm C18(2), 250 mm x 21.2 mm LC column) using gradient elution (5-95% Buffer B over 45 minutes; Buffer A dH_2O + 0.1% (v/v) TFA, Buffer B CH_3CN + 0.1% (v/v) TFA). Appropriate fractions were combined and lyophilized yielding 4.3 mg of light purple solid (68% yield) Purified products were confirmed by electrospray ionization mass spectrometry. HPLC chromatograms and mass spectra are shown in **Supplemental Figure S22**.

Chloroalkane azide synthesis

Chloroalkane carboxylic acid was first synthesized as previously described⁵ and chloroalkane azide was then synthesized from chloroalkane carboxylic acid and 3-Azido-1-propanamine (See Scheme below).



Synthesis scheme for chloroalkane azide

To synthesize chloroalkane azide, 200 mg of Chloroalkane carboxylic acid was dissolved in DMF (2 mL), 1.1 equivalents of DIEA , and 1.1 equivalents HBTU were added followed by the addition of 1.2 equivalents of freshly prepared 3-Azido-1-propanamine. The resulting mixture was rotated at room temperature for 2 hours and purified by reverse phase preparative HPLC (Luna Phenomenex, 5 μm C18(2), 250 mm x 21.2 mm LC column) using gradient elution (10-95% Buffer B over 35 minutes; Buffer A dH_2O + 0.1% (v/v) TFA, Buffer B CH_3CN + 0.1%

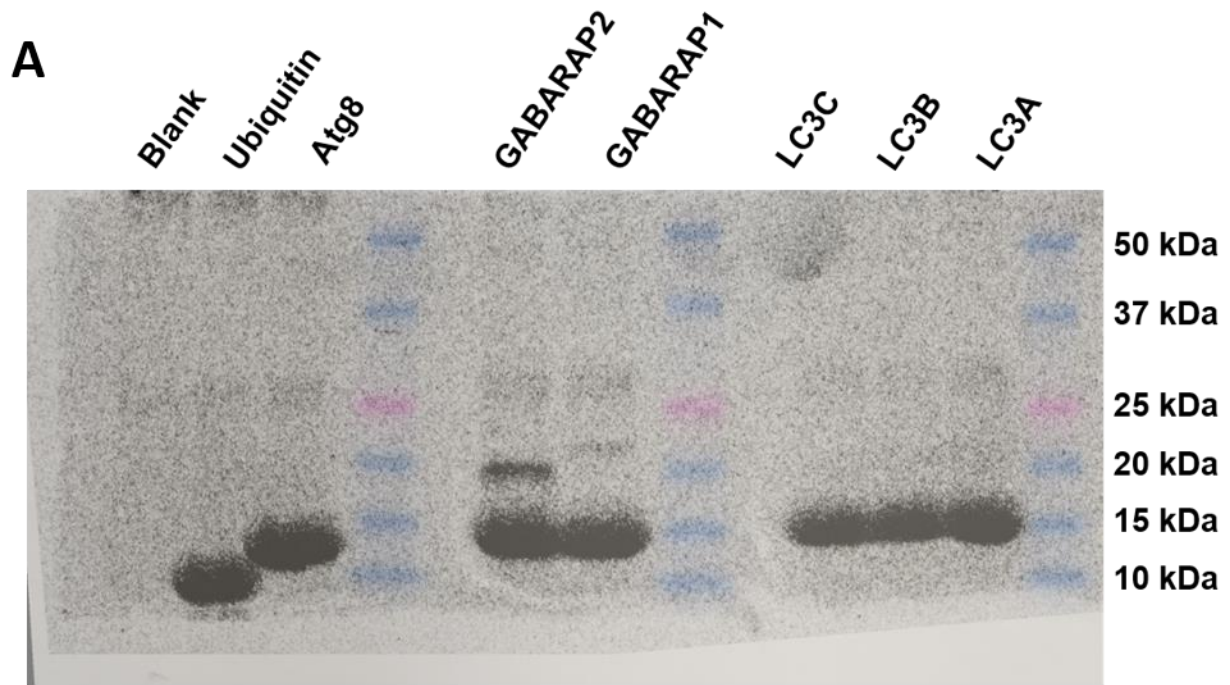
(v/v) TFA). Appropriate fractions were combined and lyophilized yielding a white solid. Purified products were confirmed by electrospray ionization mass spectrometry. HPLC chromatograms and mass spectra for each peptide may be found in the **Supplemental Figures S24**.

Synthesis of chloroalkane-labeled SUPR peptides

Copper-catalyzed click chemistry was used to conjugate chloroalkane azide to the side-chain alkyne of the C-terminal propargylglycine residue in SUPR peptides. Between 5-10 μmol of each peptide and 1.2 equivalents of chloroalkane azide were dissolved in DMF and 200 μL click solution (16 mg/mL $\text{CuSO}_4 \cdot 2\text{H}_2\text{O}$ and 30 mg/mL L-ascorbic acid in dH_2O), 5 μL of tris-(benzyltriazolylmethyl)amine (TBTA, 100 mg/mL in DMF) were added. Reaction mixture was brought to a final volume of 500 μL with dH_2O and rotated at room temperature for 2 hours and purified by reverse phase preparative HPLC (Luna Phenomenex, 5 μm C18(2), 250 mm x 21.2 mm LC column) using gradient elution (10-95% Buffer B over 35 minutes; Buffer A dH_2O + 0.1% (v/v) TFA, Buffer B CH_3CN + 0.1% (v/v) TFA). Appropriate fractions were combined and lyophilized yielding a white solid. Purified products were confirmed by electrospray ionization mass spectrometry. HPLC chromatograms and mass spectra for each peptide may be found in the **Supplemental Figures S25, S26, S27, and S28**.

A₅₇₀ Absorbance	Cisplatin Presence			Peptide Structure			Cisplatin Presence x Peptide Structure Interactions		
	df	F	p	df	F	p	df	F	p
OVAR8	1,56	1651.70	< 0.0001	3,56	62.85	< 0.0001	3, 56	11.41	< 0.0001
HEY	1, 55	399.849	< 0.0001	3, 55	23.964	< 0.0001	3, 55	1.222	0.31
Tumor Weight	Carboplatin Presence			Peptide Structure			Carboplatin Presence x Peptide Structure		
	df	F	p	df	F	p	df	F	p
Trial 1	1, 25	24.04	< 0.001	1, 25	15.389	0.0006	1, 25	10.899	0.0029
Trial 2	1,52	92.507	< 0.0001	2, 52	20.382	< 0.0001	2, 52	11.868	< 0.0001

Table S1: Statistical Parameters obtained from analysis of data from Figures 6 and 7. Results of two-way ANOVA with type I (cellular viability measurements) or type III (tumor weight measurements) sum of squares tests to determine the independent and interactive effects of platinum and anti-autophagy treatments.



B

Atg8 homologue	Area (a.u)	Relative Density
LC3A	55645.86	1
LC3B	51706.78	0.929212
LC3C	50639.13	0.910025
GABARAP1	60878.65	1.094037
GABARAP2	62433.28	1.121975
Atg8	59728.73	1.073372
Ubiquitin	50974.14	0.916046

Figure S1: SDS-PAGE and Autoradiography of *in vitro* translated Atg8 homologs. **A)** Autoradiograph of SDS-PAGE gel showing the molecular weights of *in vitro* translated proteins. **B)** Quantitation of band intensity by ImageJ. These values were used to normalize the bound counts in **Figure 4B** of the manuscript.

LC3C	MPPPQKIPSVRPFKQRKSLAIRQEEVAGIRAKFPNKIPVVVERYPRETFLPPLDKTKFLV
LC3A	-----MPSDRPFKQRRSFADRCKEVQQIRDQHPSKIPVIERYKGEKQLPVLDKTKFLV
LC3B	-----MPSEKTFKQRRTFEQRVEDVRLIREQHPTKIPVIERYKGEKQLPVLDKTKFLV
Atg8	-----MKSTFKSEYPF EKRKAE SERIADR FKNRIPV ICEKAEK-SDIPEIDKRKYL
GABARAPL1	-----MKFQYKEDHPFEYRKKEGEKIRKKYPDRVPVIVEKAPK-ARVPDLDKRKYLV
GABARAPL2	-----MKWMFKEDHSL EHRCVE SAKIRAKYPDRVPVIVEK VSG-SQIVDIDKRKYL
LC3C	PQELTMTQFLSIIRSRMVLRATEAFYLLVNNKSLVSM SATMAEIYRDYKDEDGFVYMTYA
LC3A	PDHVNMSSELVKIIRRLQLNPTQAFLLVNQHSMVSVSTPIADIYEQEKDEDGFLYMYA
LC3B	PDHVNMSSELIKIIRRLQLNANQAFLLVNGHSMVSVSTPISEVYESEKDEDGFLYMYA
Atg8	PADLTVGQFVYVIRKRIMLPPEKAI FIFVNDT-LPPTAALMSAIYQEHKDKDGFLYVYS
GABARAPL1	PSDLTVGQFYFLIRKRIHLRPEDALFFFVNNT-IPPTSATMGQLYEDNHEEDYFLYVAYS
GABARAPL2	PSDITVAQFMWIIRKRIQLPSEKAI FLFVDKT-VPQSSLTMGQLYEKEKDEDGFLYVAYS
LC3C	SQETFGCLESAAPRDGSSLEDRPCNPL
LC3A	SQETFGF-----
LC3B	SQETFGMKLSV-----
Atg8	GENTFGR-----
GABARAPL1	DESVYGK-----
GABARAPL2	GENTFGF-----

Figure S2: Protein Sequence alignment of LC3A, LC3B, LC3C, GABARAPL1, GABARAPL2, and Atg8. Alignment was performed in Clustal Omega. Identical residues are shown in red, similar residues are shown in pink, and non-similar residues are shown in black.

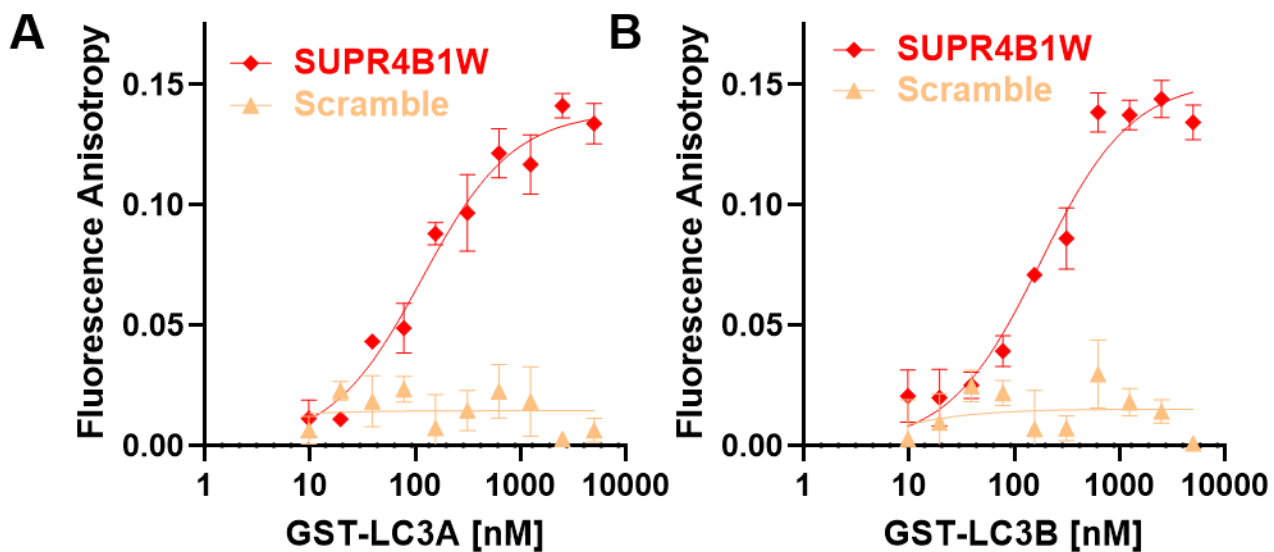
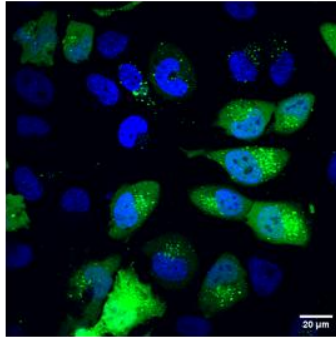
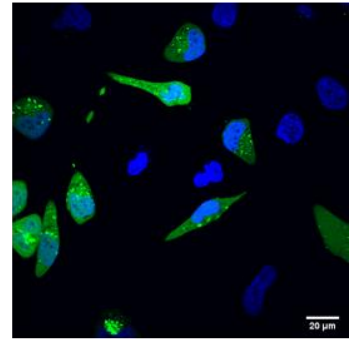
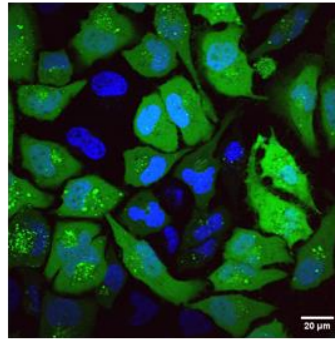
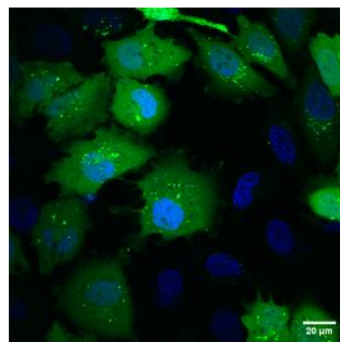
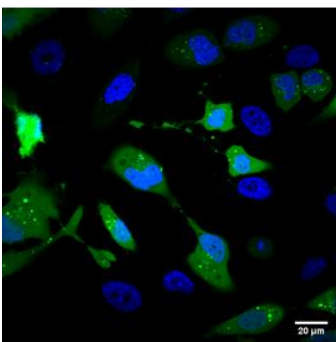


Figure S3: Binding of SUPR4B1W and scrambled SUPR4B1W to LC3A and LC3B. **A)** SUPR4B1W bound to LC3A with a $K_D = 116.1 \pm 14$ nM by FP while the scrambled peptide showed no binding at concentrations as high as 5 μ M. **B)** SUPR4B1W bound to LC3B with a $K_D = 176.6 \pm 23.8$ nM while the scrambled peptide showed no binding at concentrations as high as 5 μ M.

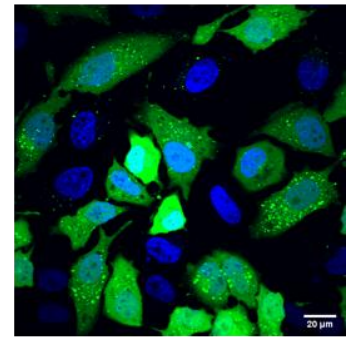
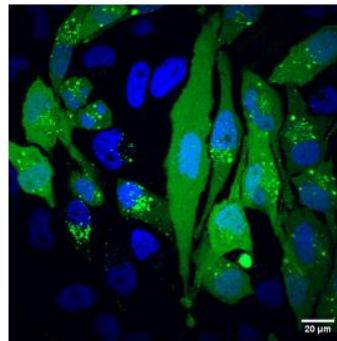
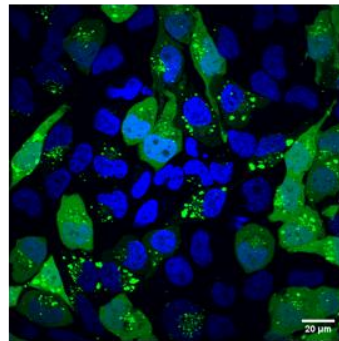
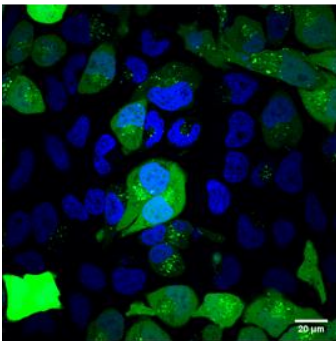
No Treatment



SUPR4B1W



Scrambled



500 μ M

50 μ M

5 μ M

500 nM

Figure S4: Representative Fluorescence Microscopy Images from Figure 6D. HeLa cells expressing eGFP-LC3 were treated with the indicated concentration of SUPR4B1W or SUPR4B1W scrambled for 24 h followed by starvation for 2 h. The cells were fixed, mounted, sealed with coverslips and imaged. Green = GFP-LC3, Blue = DAPI. Magnification = 60X.

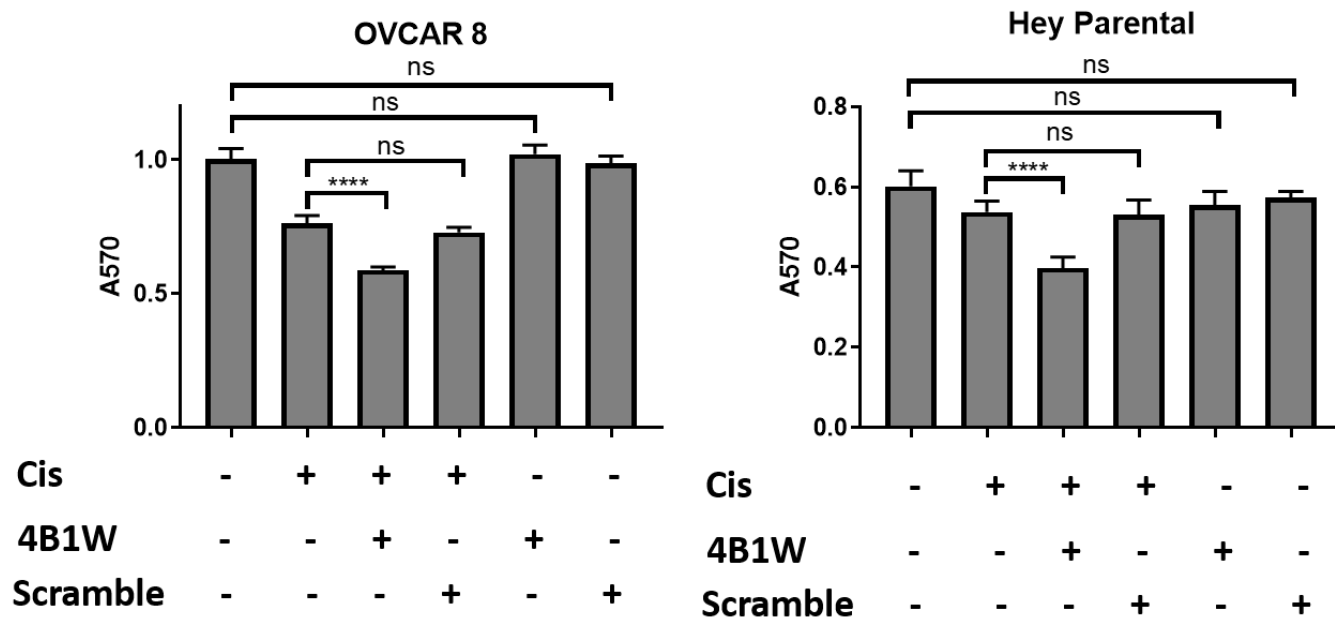


Figure S5: Scrambled SUPR4B1W does not affect cellular viability. Treatment of OVCAR8 and Hey cell lines with a scrambled version of SUPR4B1W in which the amino acid order has been randomized does not impact cellular viability after 48 hours of treatment when administered alone or in combination with cisplatin. This suggest that the viability change induced by SUPR4B1W is the effect of a specific interaction and not general toxicity due to peptide uptake.

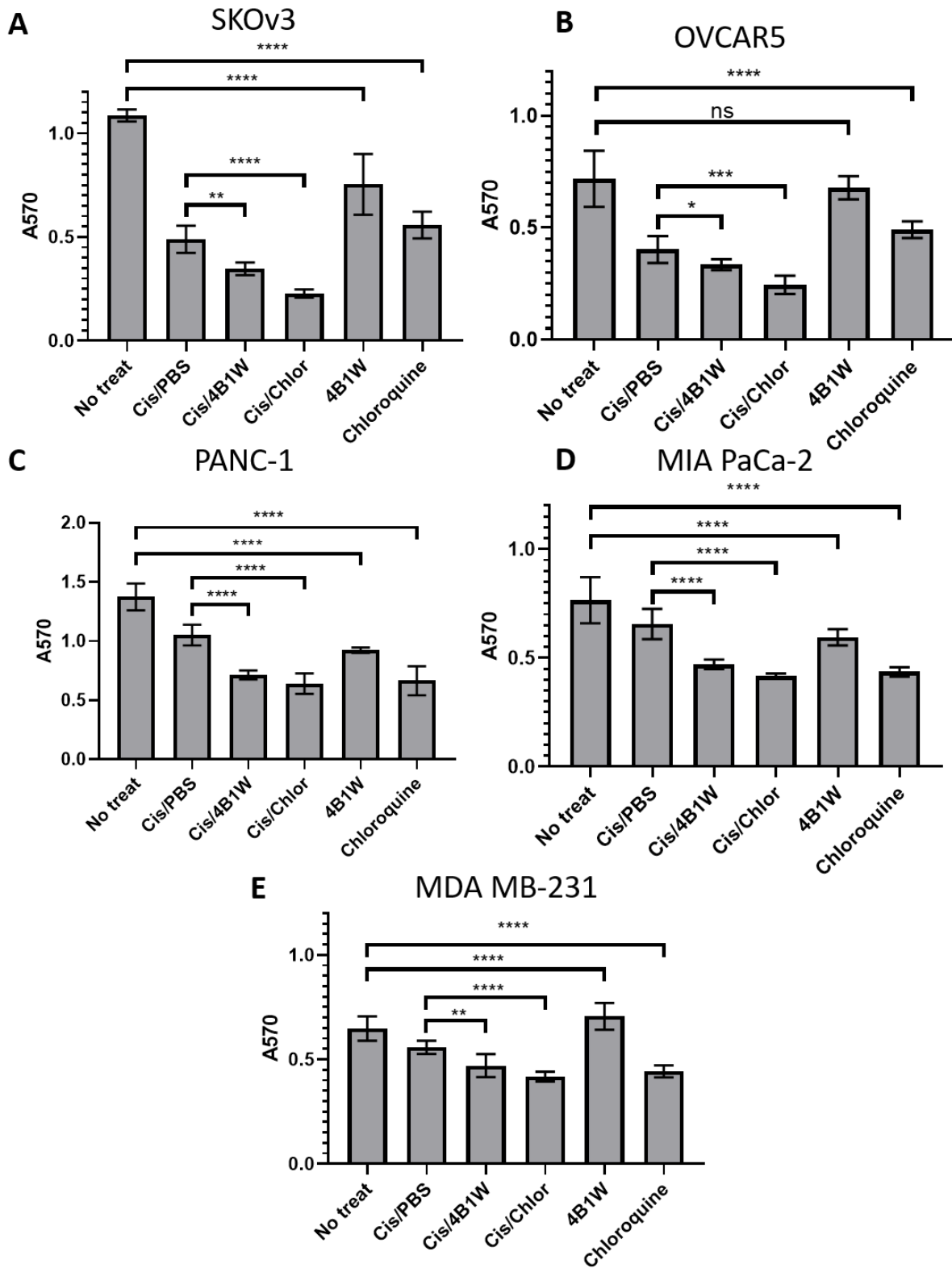
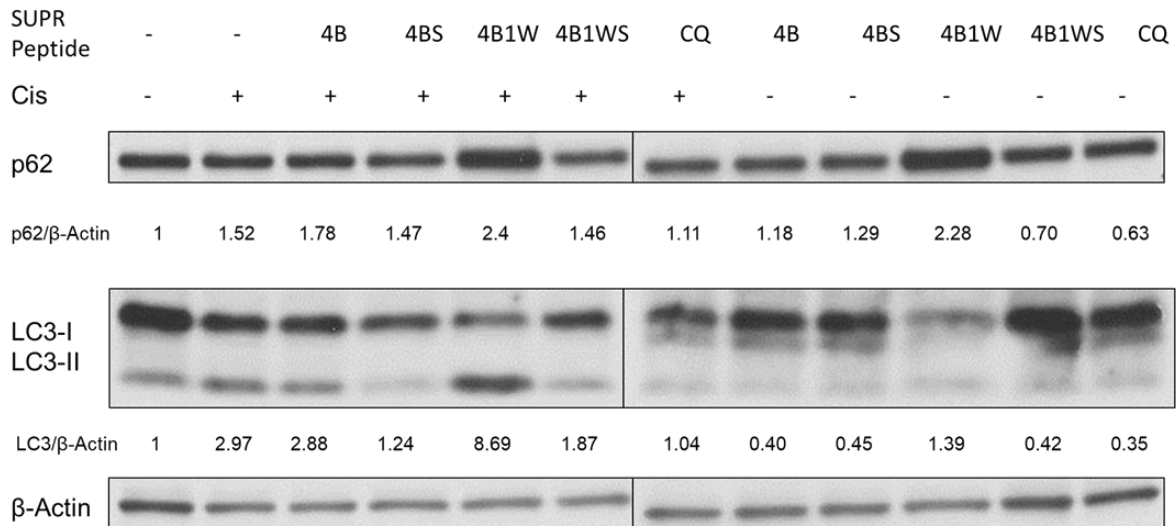


Figure S6: SUPR4B1W sensitizes ovarian, pancreatic, and breast cancer cell lines to cisplatin *in vitro*. Treatment of SKOV3 (A), OVCAR5 (B), PANC-1 (C), MIA PaCa-2 (D), and MDA MB-231 (E) cancer cells with SUPR4B1W and cisplatin significantly reduces cell viability after 48 h relative to cisplatin alone.

A Cisplatin Sensitization in OVCAR 8



B Cisplatin Sensitization in HEY

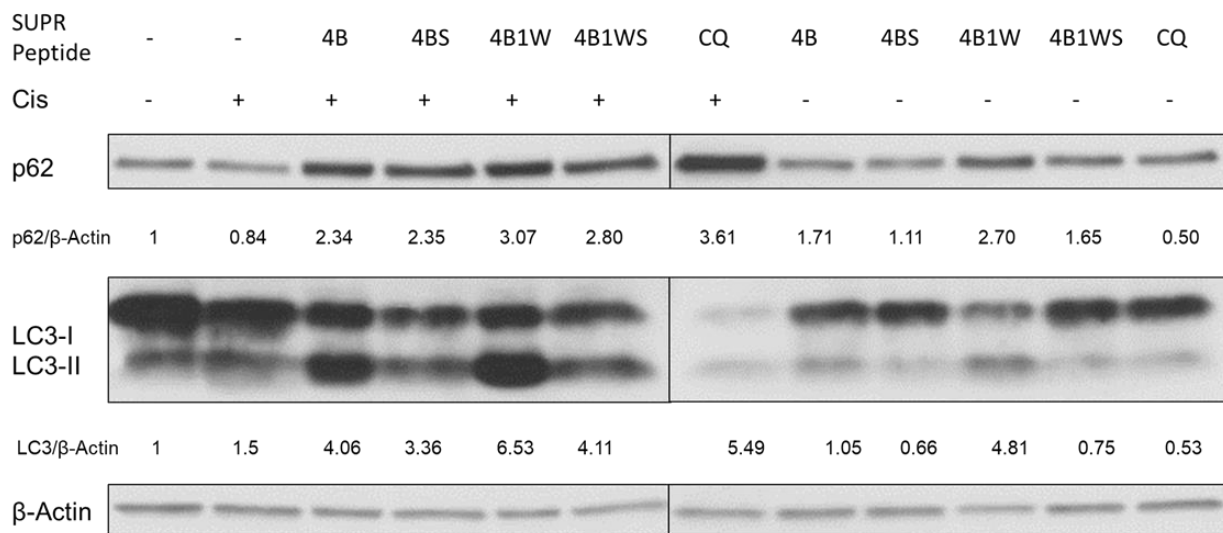
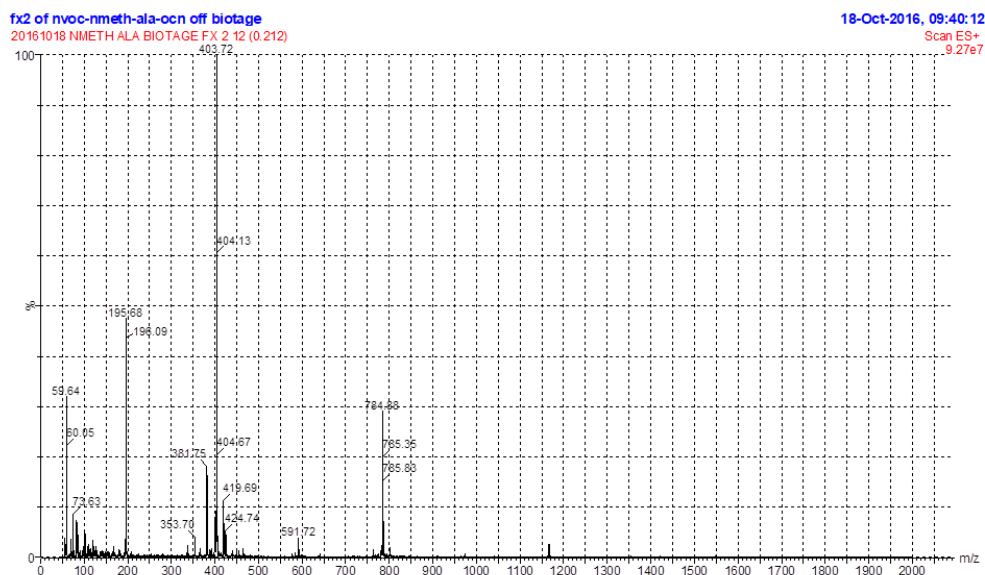


Figure S7: Extended version of Figure 6. These western blots show treatment of OVCAR8 (A) and HEY (B) ovarian cancer cells with SUPR peptides in the presence and absence of cisplatin. Note – the left blots are reproduced here from Figure 6 while the right side blots show the effect of cisplatin and chloroquine (CQ) as well as the effects of SUPR peptides and CQ in the absence of cisplatin. Here we show that combined treatment with cisplatin and CQ ablates LC3II levels rather causing LC3II accumulation as was seen when SUPR4B1W was combined with cisplatin. This suggests that the mechanism of autophagy inhibition with SUPR4B1W differs from that of CQ. Treatment with SUPR peptides in the absence of cisplatin does not result in significant accumulation of LC3II although some accumulation of p62 is observed in the case of SUPR4B1W in HEY.

A NVOC-N-Methyl-L-Alanine OCN



B pdCpA-N-Methyl-L-Alanine-NVOC

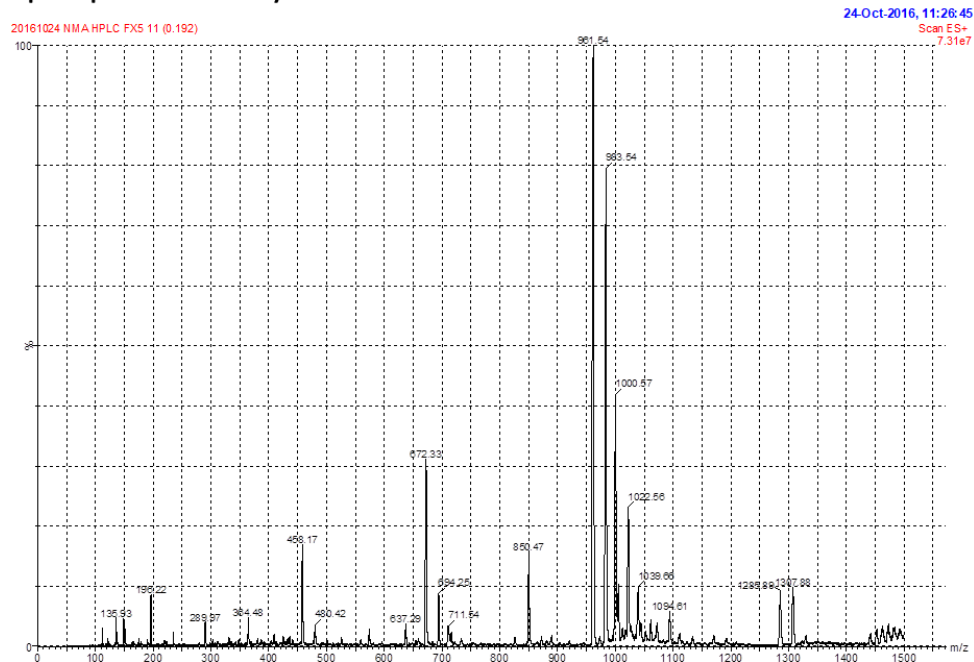


Figure S8. Electrospray ionization mass spectrometry of NVOC-N-Methyl-L-alanine-OCN and pdCpA-N-Methyl-L-alanine-NVOC. **A)** NVOC-N-Methyl-L-alanine-OCN product was confirmed by observing peaks for $[M+H]^+$ (expected 382.13, observed 381.75), $[M+Na]^+$ (expected 404.11, observed 404.12), and $[2M+Na]^+$ (expected 785.23, observed 785.35). **B)** pdCpA-N-Methyl-L-alanine-NVOC product was confirmed by observing peaks for $[M+H]^+$ (expected 961.22, observed 961.54) and $[M+Na]^+$ (expected 983.20, observed 983.54)

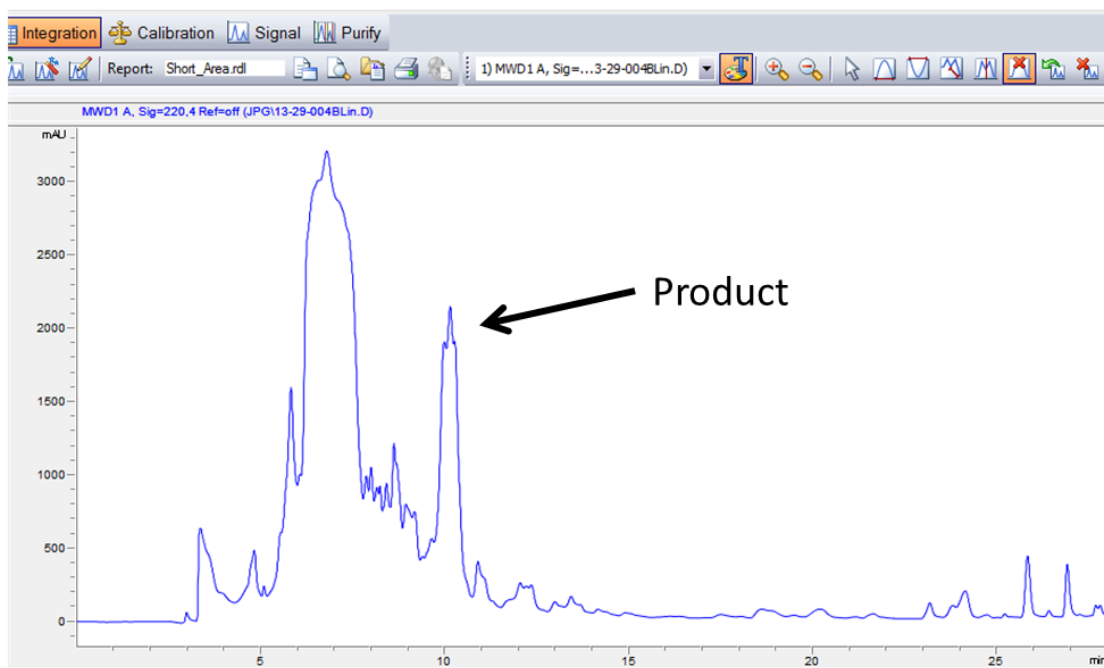
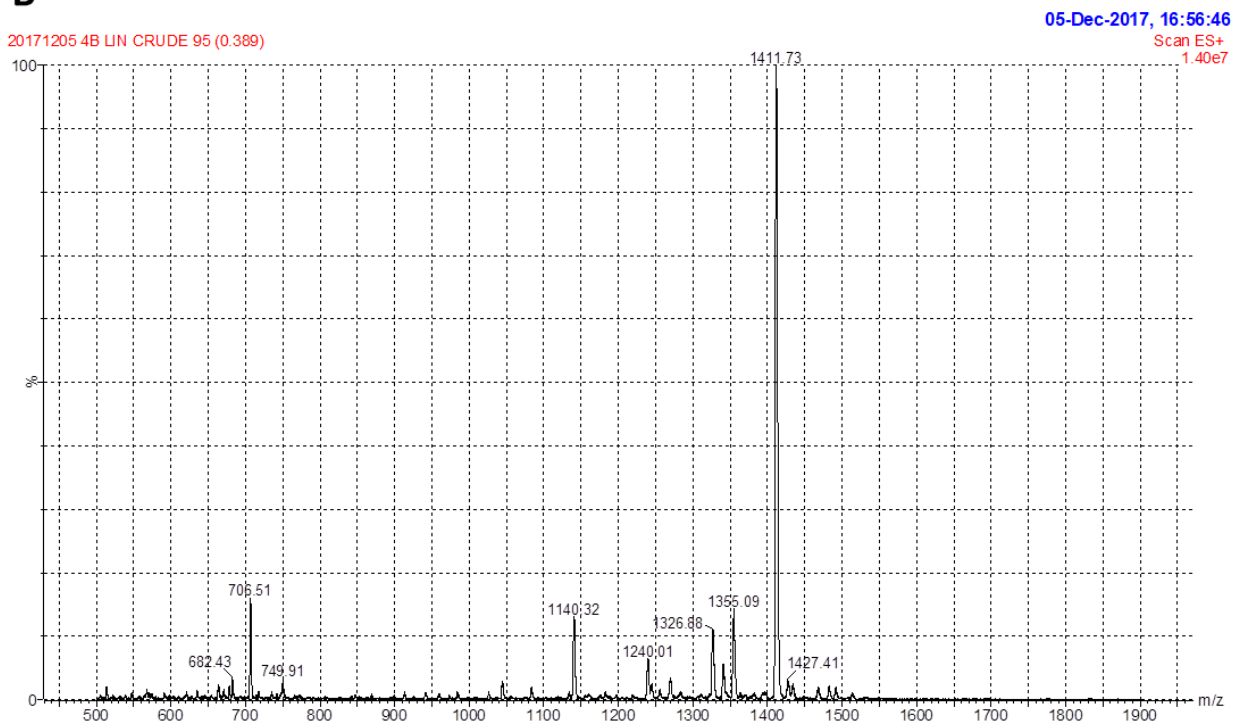
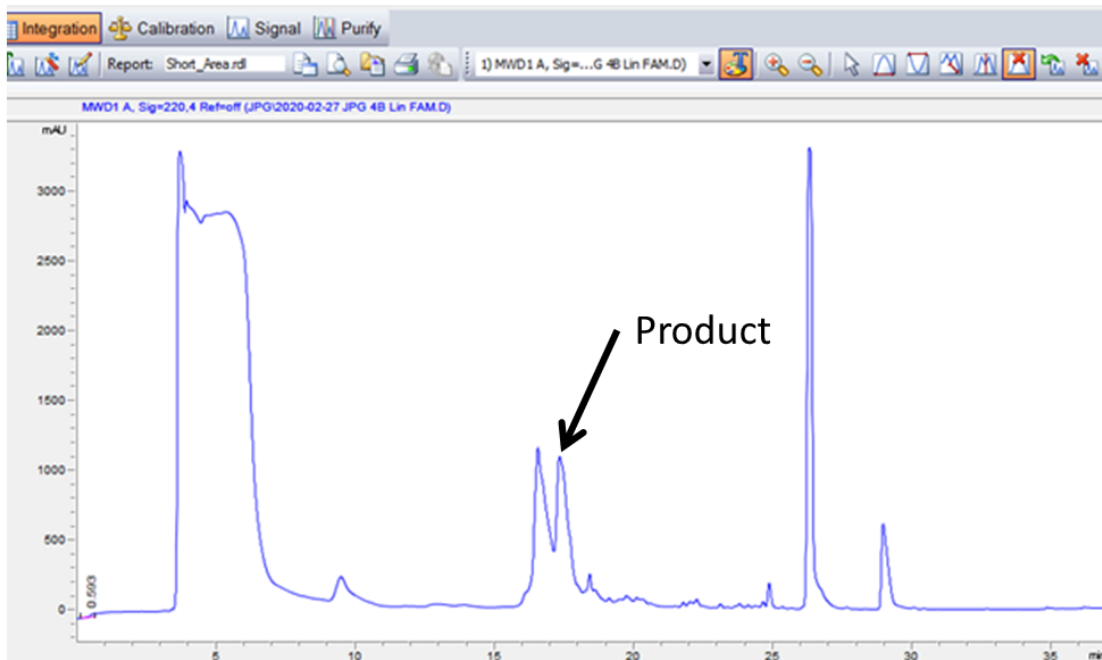
A**B**

Figure S9: SUPR4B (Linear). **A)** Preparative HPLC purification (A_{220}) of crude product (5-95% ACN over 30 min) **B)** Electrospray ionization mass spectroscopy. The product was confirmed by observing peaks corresponding to $[M+H]^+$ (expected 1411.67, observed 1411.73) and $[M+2H]^{2+}$ (expected 706.34, observed 706.51)



B

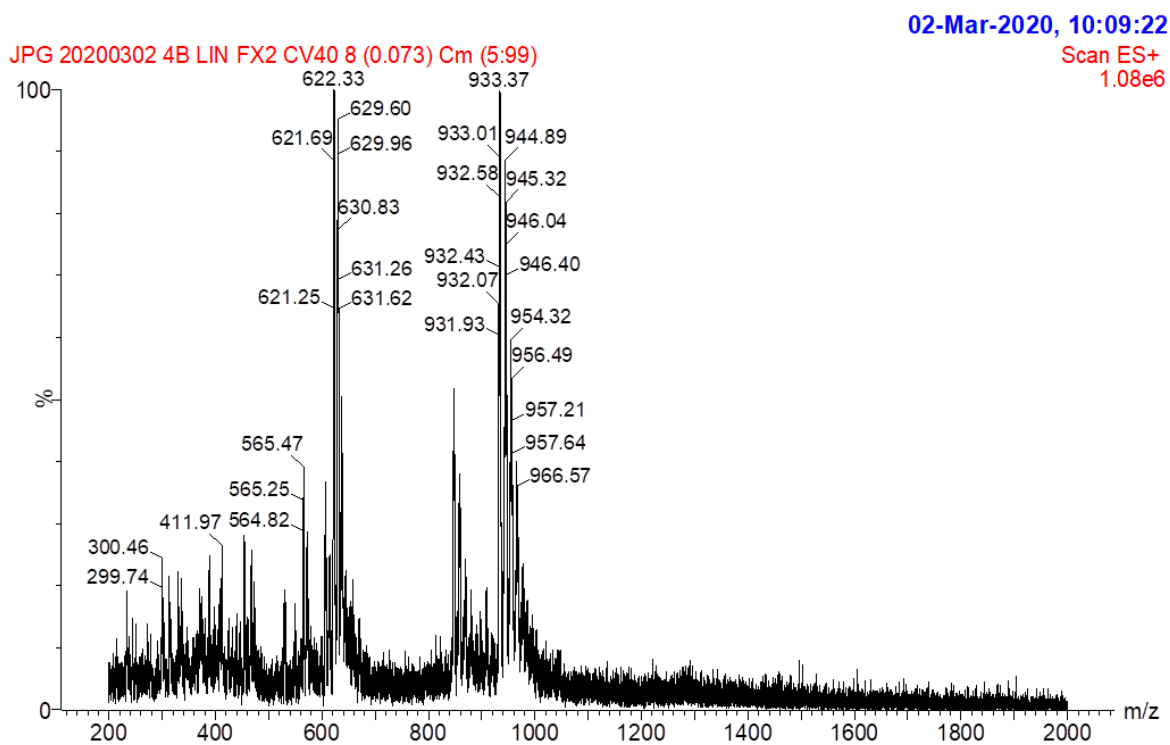


Figure S10: SUPR4B-fluorescein (linear). **A)** Preparative HPLC (A_{220}) purification of crude product (5-60% ACN over 30 min) **B)** Electrospray ionization mass spectrometry. The product was confirmed by observing peaks corresponding to $[M+2H]^{2+}$ (expected 934.82, observed 933.37) and $[M+3H]^{3+}$ (expected 623.55, observed 622.33)

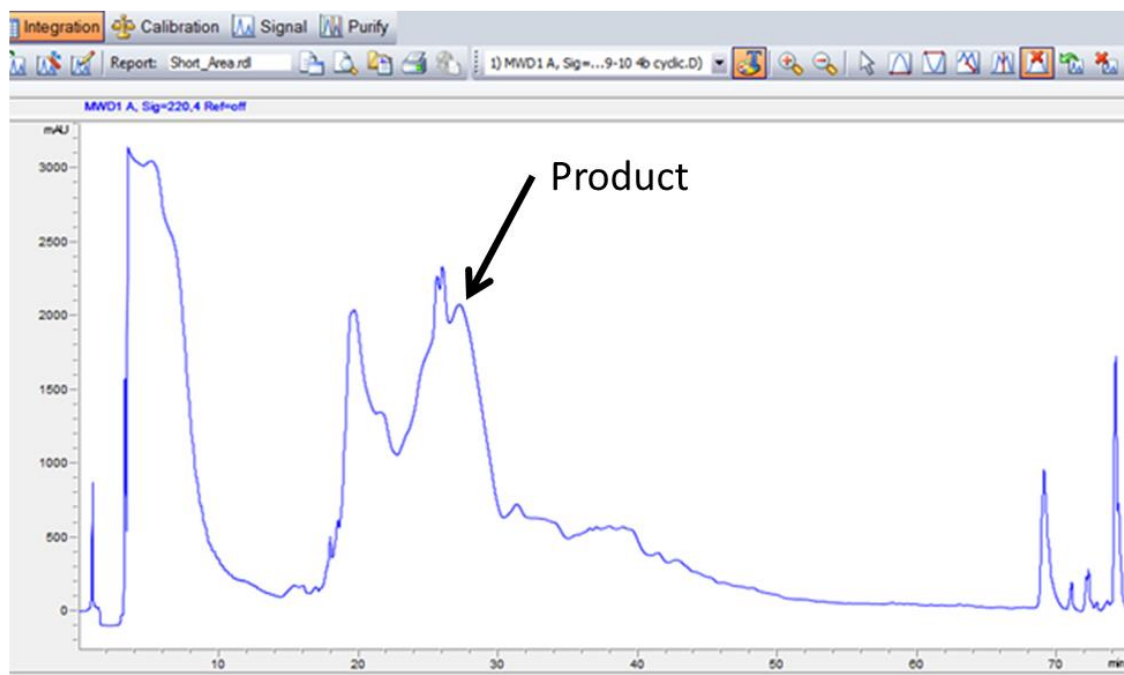
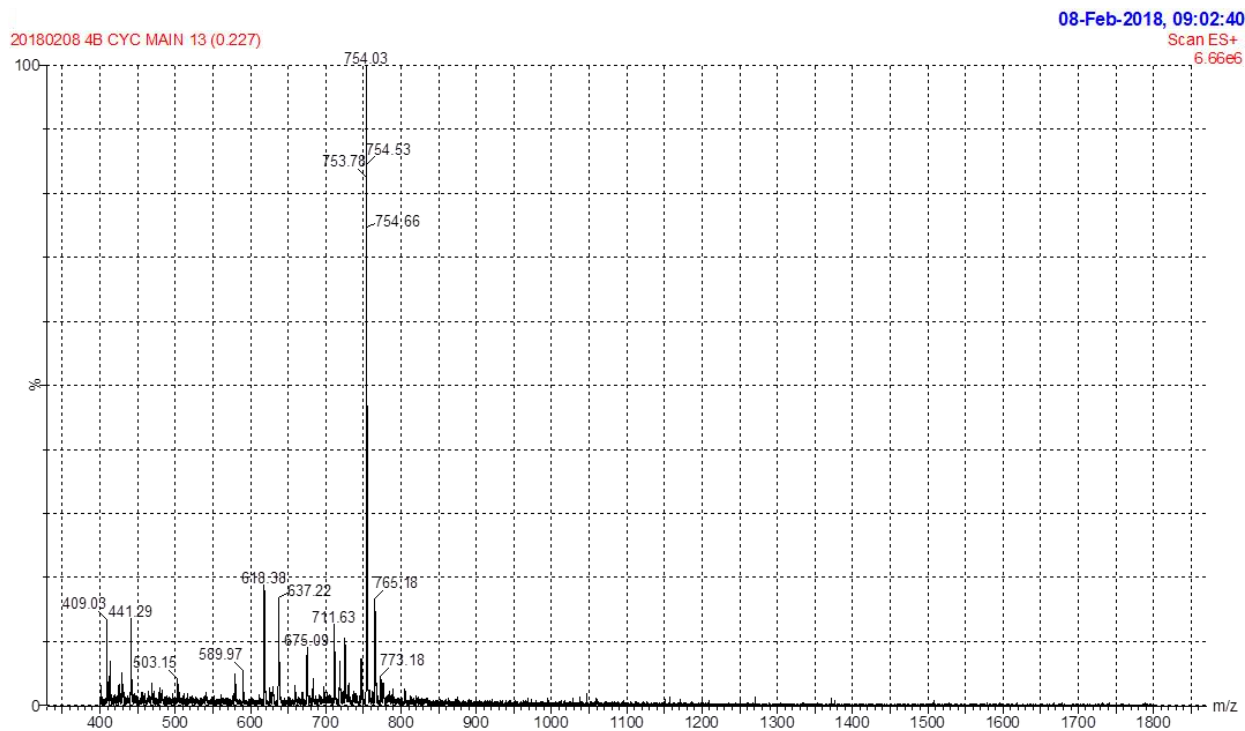
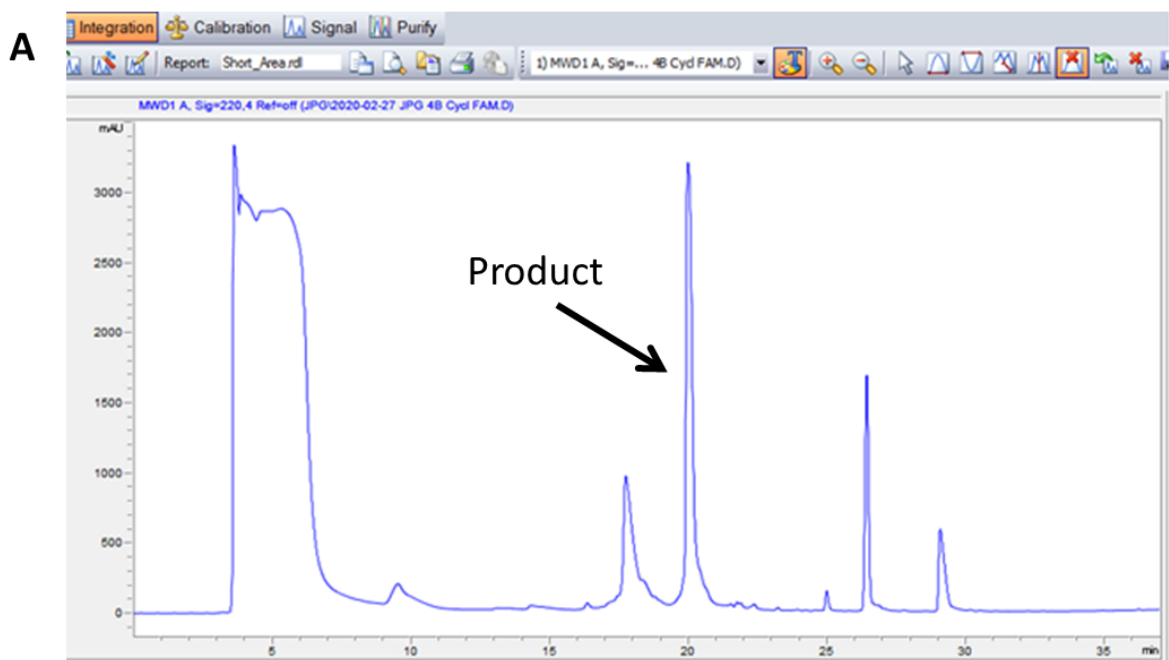
A**B**

Figure S11: SUPR4B (Cyclic). **A)** Preparative HPLC purification (A₂₂₀) of crude product (20-60% ACN over 60 min) **B)** Electrospray ionization mass spectrometry. The product was confirmed by observing peaks corresponding to [M+2H]²⁺ (expected 753.88, observed 754.03)



B

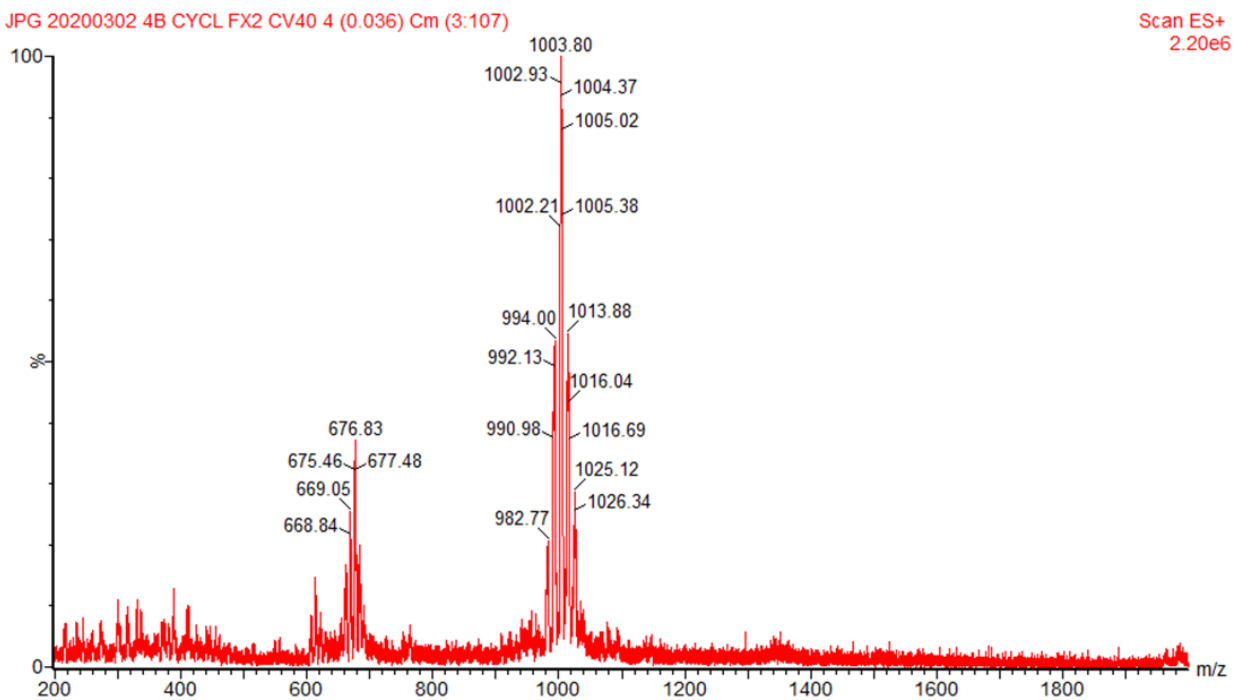


Figure S12: SUPR4B-fluorescein (cyclic). **A)** Preparative HPLC (A_{220}) purification of crude product (5-95% ACN over 30 min) **B)** Electrospray ionization mass spectroscopy. The product was confirmed by observing peaks corresponding to $[M+3Na]^+$ (expected 677.61, observed 676.83), $[M+H+Na]^{2+}$ (expected 993.93, observed 994.00), and $[M+2Na]^{2+}$ (expected 1004.92, observed, 1004.37)

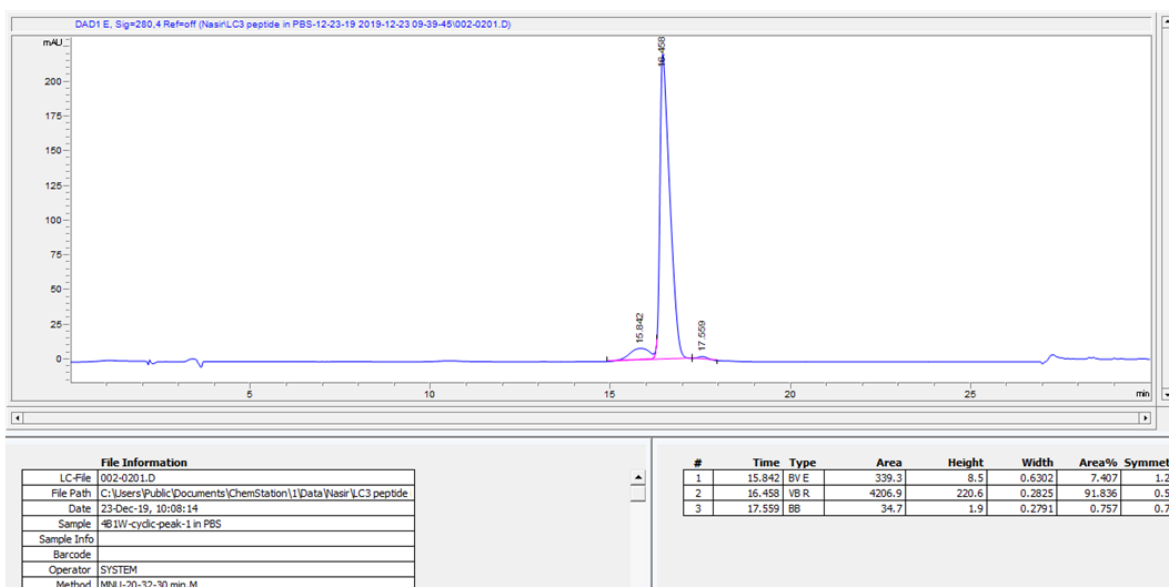
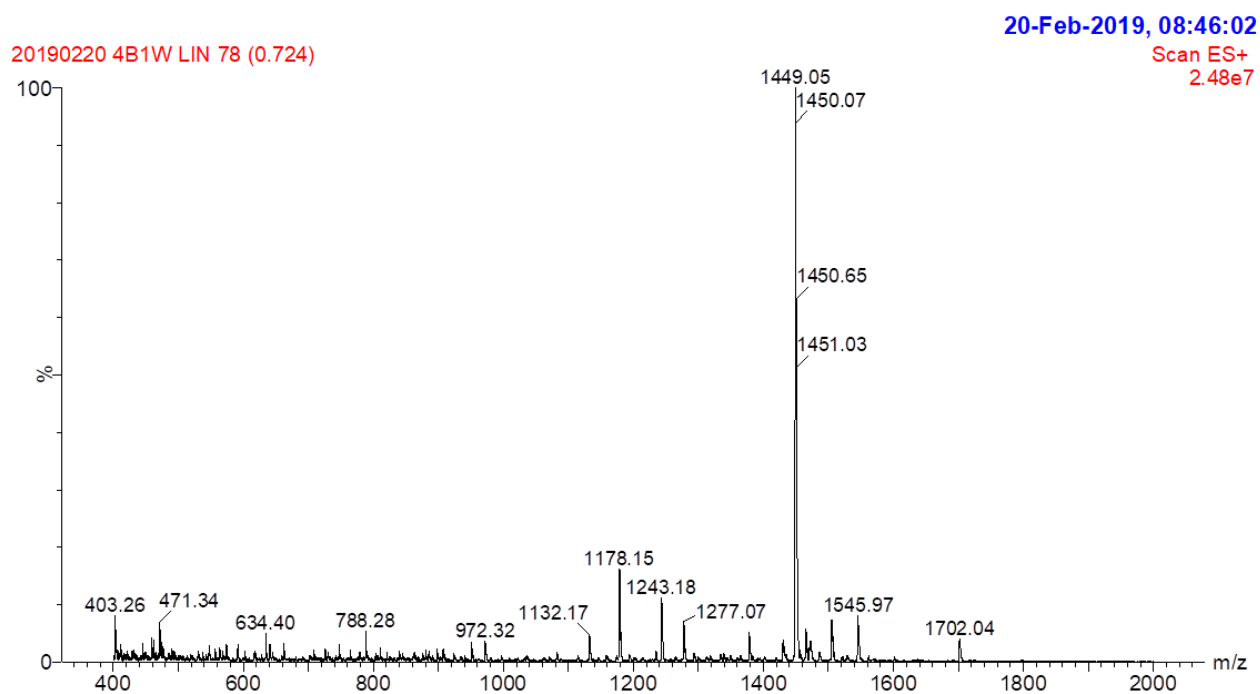
A**B**

Figure S13: SUPR4B1W (Linear). **A)** Analytical HPLC trace (A_{280}) of purified product (10-30% ACN over 30 min). **B)** Electrospray ionization mass spectroscopy. The product was confirmed by observing peaks corresponding to $[M+H]^+$ (expected 1449.74, observed 1450.07)

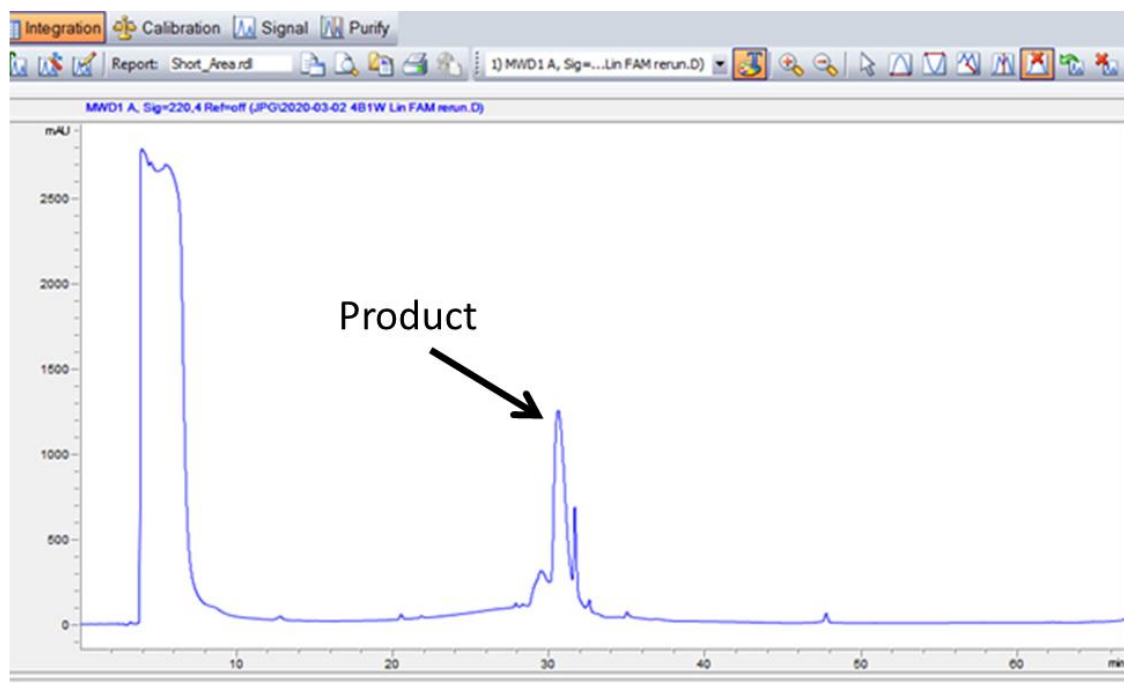
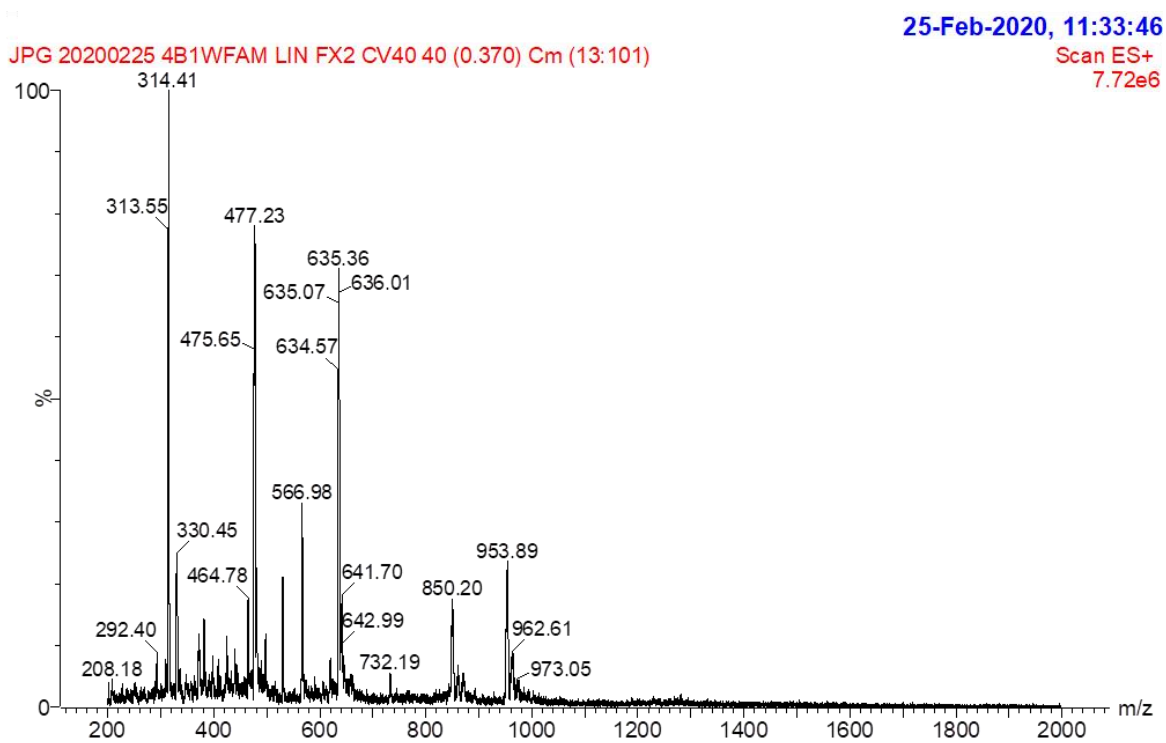
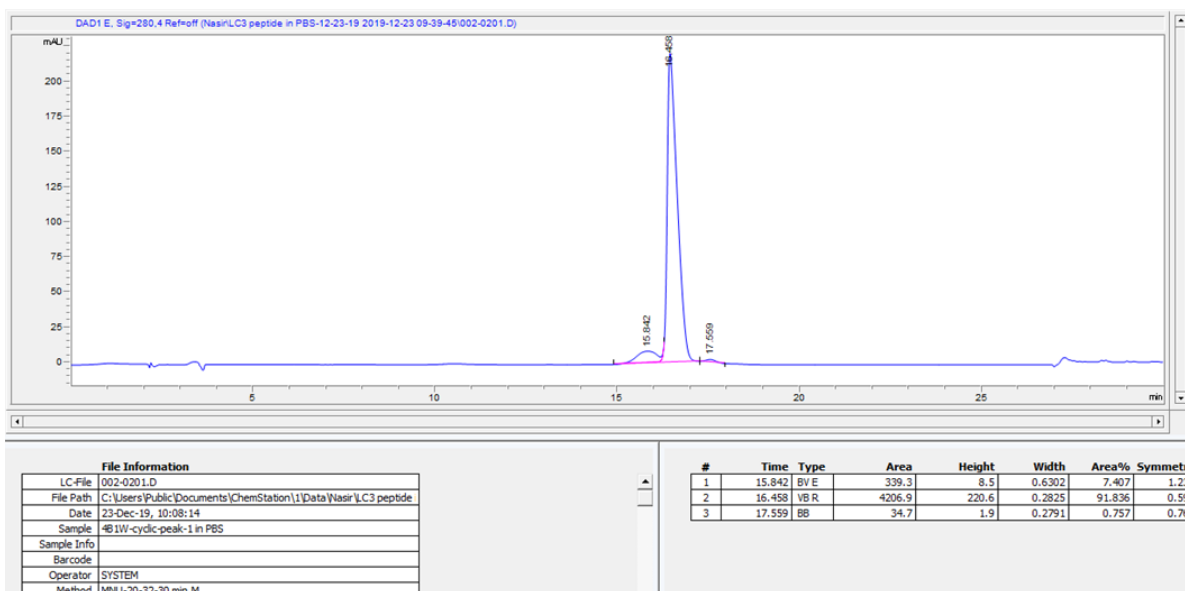
A**B**

Figure S14: SUPR4B1W-fluorescein (linear). **A)** Preparative HPLC purification (A_{220}) of crude product (5-95% ACN over 60 min). **B)** Electrospray ionization mass spectroscopy. The product was confirmed by observing peaks corresponding to $[M+2H]^{2+}$ (expected 954.43, observed 953.89), $[M+3H]^{3+}$ (expected 636.62, observed 636.01), and $[M+4H]^{4+}$ (expected 477.72, observed 477.23)

A**B**

20190307 4B1W CYCL FX5 28 (0.255)

07-Mar-2019, 08:30:10

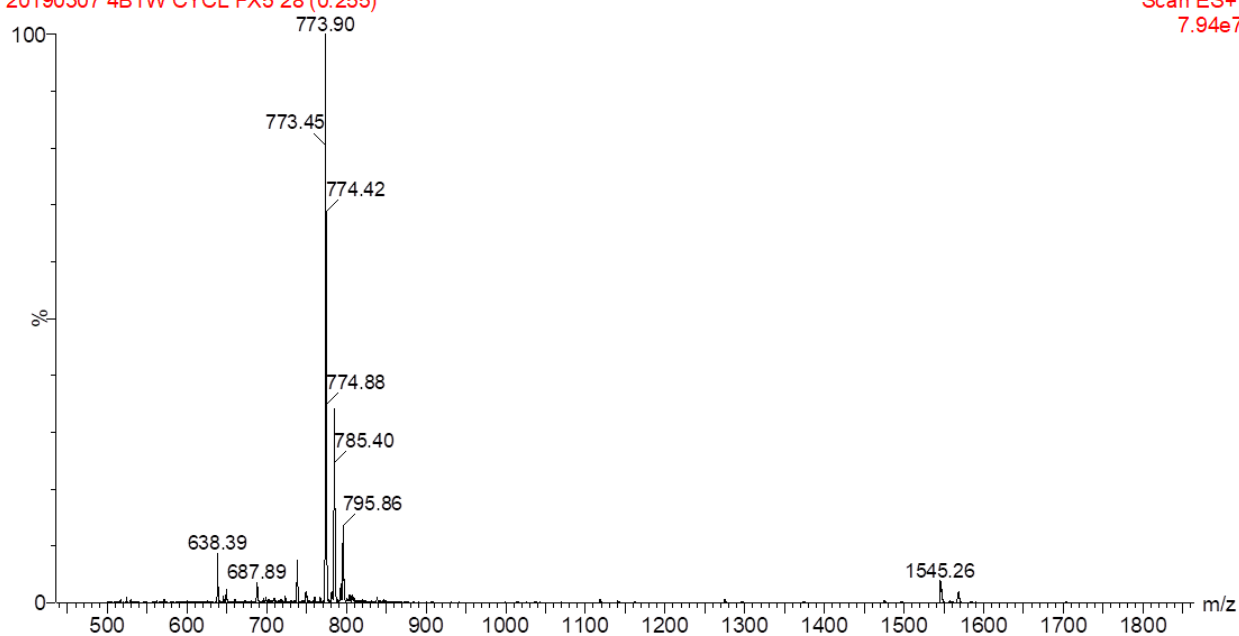
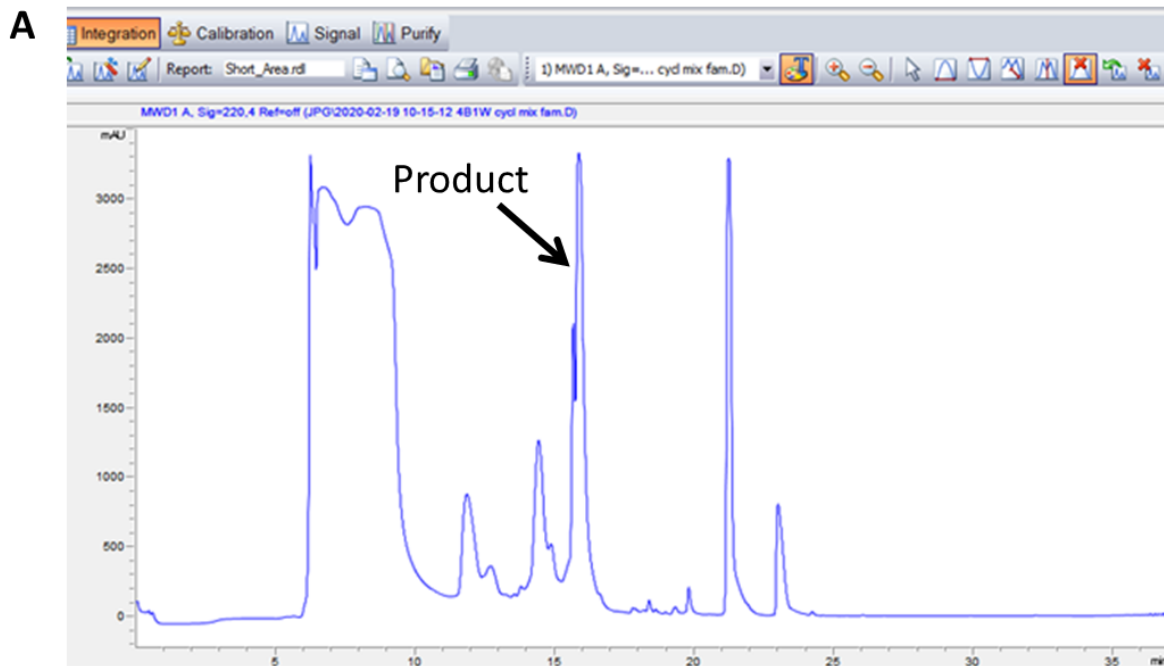
Scan ES+
7.94e7

Figure S15: SUPR4B1W (Cyclic). **A)** Analytical HPLC trace (A_{280}) of purified product (10-30% ACN over 30 min). **B)** Electrospray ionization mass spectroscopy. The product was confirmed by observing peaks corresponding to $[M+H]^+$ (expected 1545.76, observed 1544.26), $[M+2H]^{2+}$ (expected 773.38, observed 773.90), $[M+H+Na]^{2+}$ (expected 784.38, observed 785.40), and $[M+2Na]^{2+}$ (expected 795.37, observed 795.86)



B

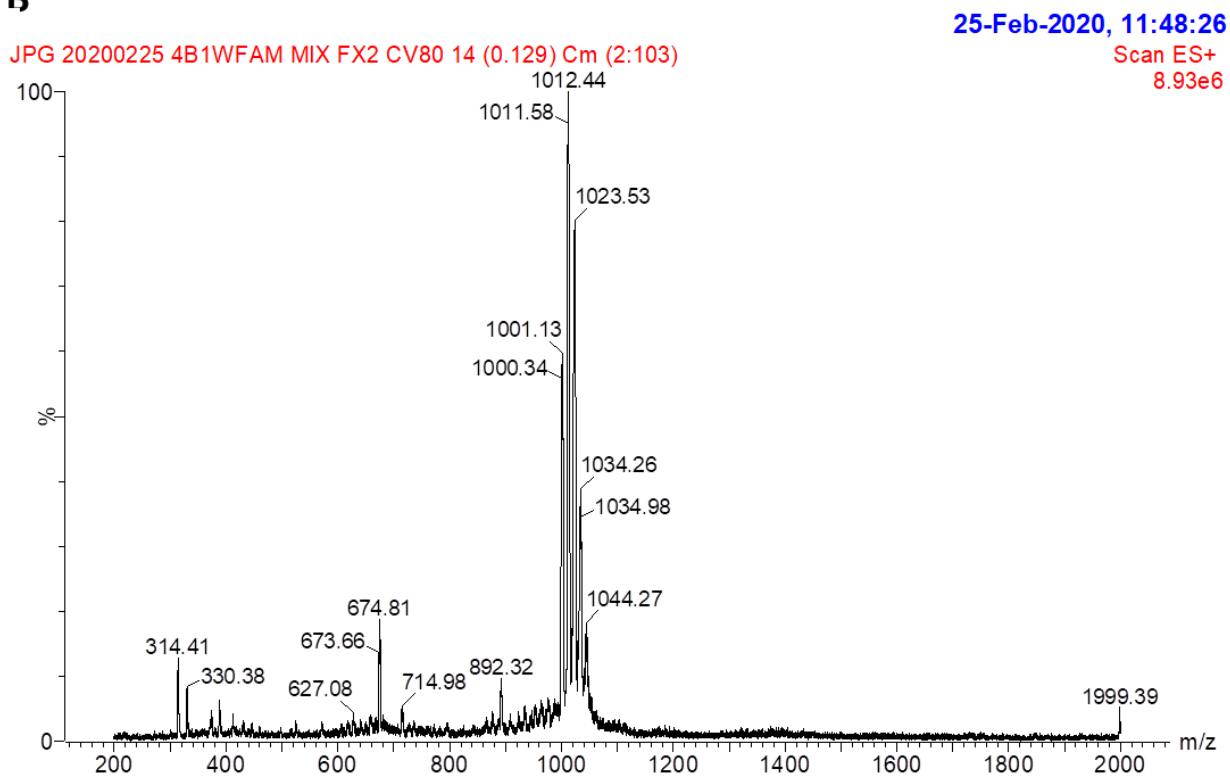


Figure S16: SUPR4B1W-fluorescein (cyclic). **A)** Preparative HPLC purification (A_{220}) of crude product (5-95% ACN over 60 min). **B)** Electrospray ionization mass spectroscopy. The product was confirmed by observing peaks corresponding to $[M+2H]^{2+}$ (expected 1002.44, observed 1001.13), $[M+H+NH_4]^{2+}$ (expected 1010.96, observed 1011.58), and $[M+2H+ACN]^{2+}$ (expected 1022.96, observed 1023.53)

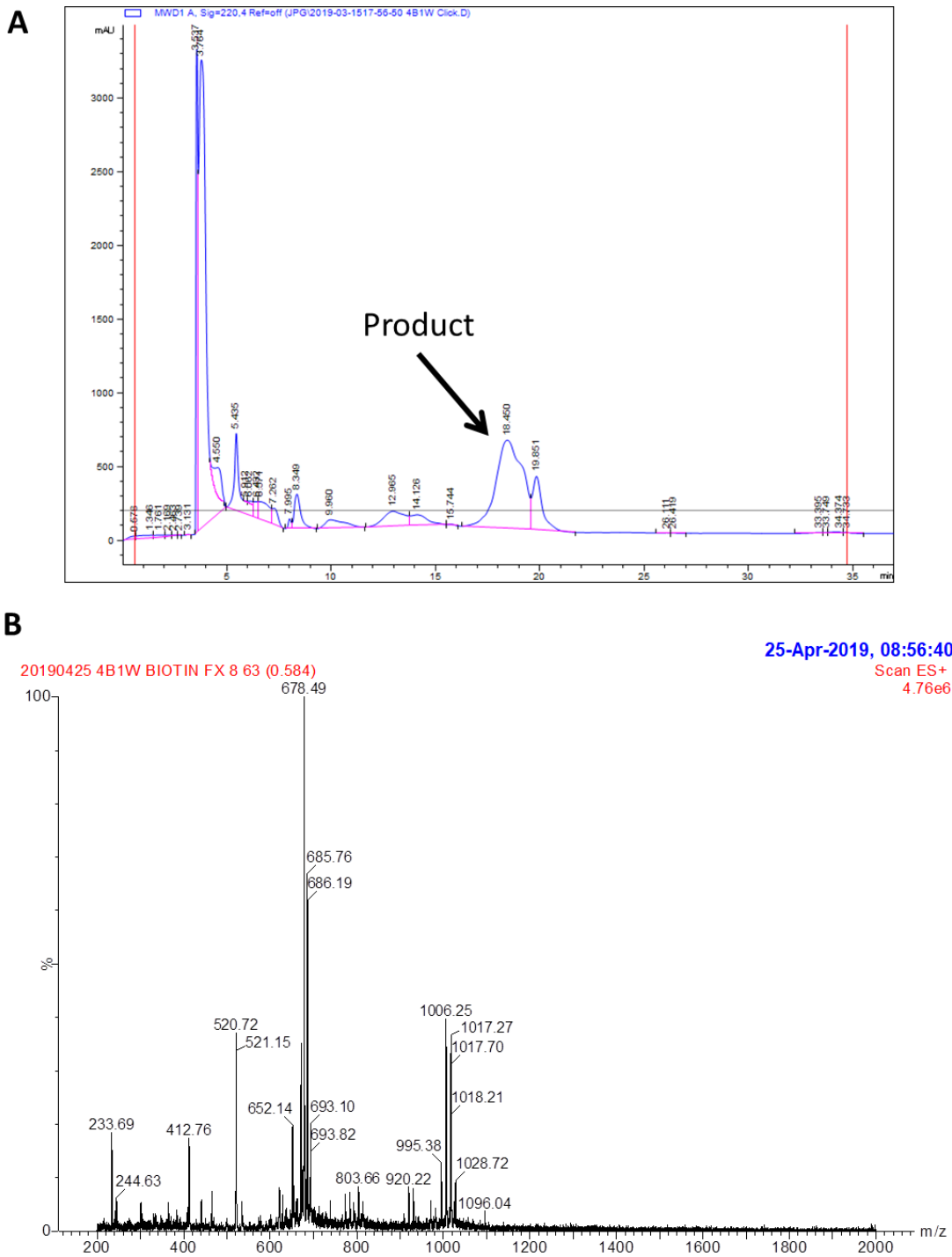


Figure S17: SUPR4B1W-biotin (cyclic). **A)** Preparative HPLC purification (A_{220}) of crude product (20-60% ACN over 30 min. **B)** Electrospray ionization mass spectroscopy. The product was confirmed by observing peaks corresponding to $[M+H+2Na]^{3+}$ (expected 678.76, observed 678.49), $[M+H+Na]^{2+}$ (expected 1006.48, observed 1006.25), and $[M+2Na]^{2+}$ (expected 1017.47, observed 1017.70)

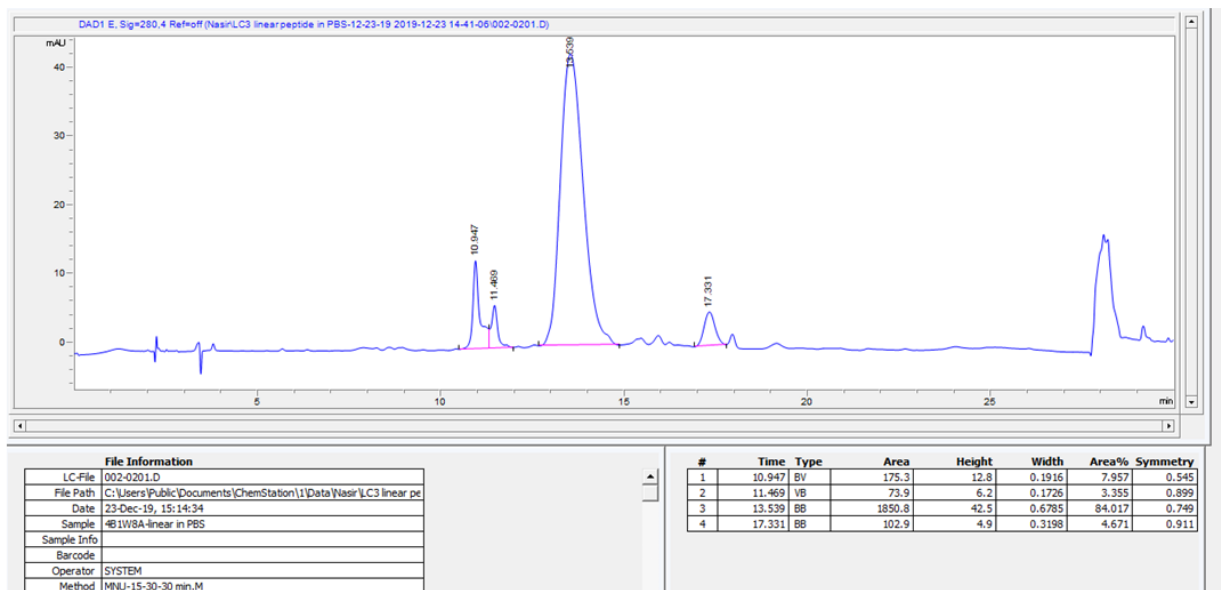
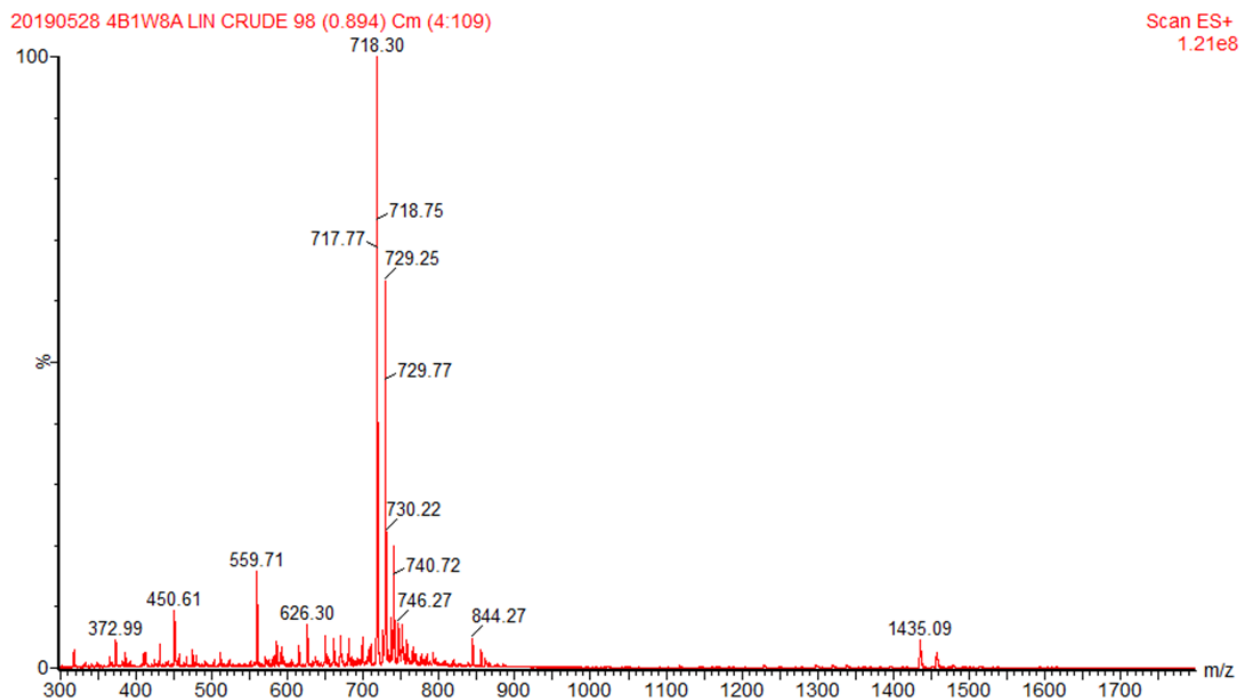
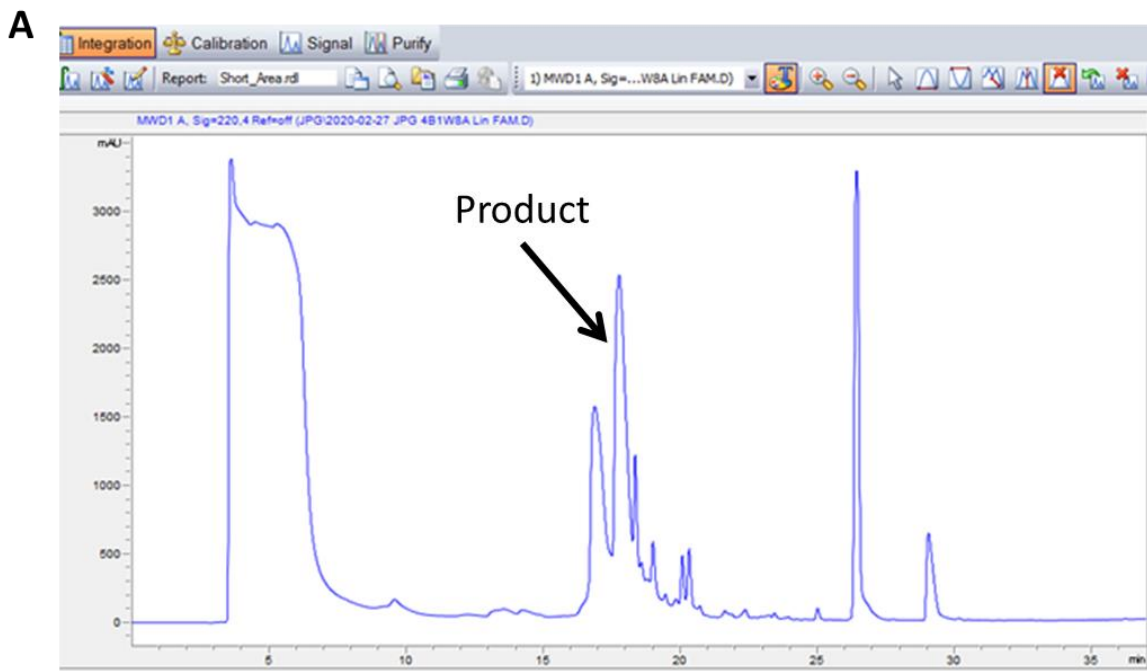
A**B**

Figure S18: SUPR4B1W8A (Linear). **A**) Analytical HPLC trace (A_{280}) of purified product (10-30% ACN over 30 min). **B**) Electrospray ionization mass spectrometry. The product was confirmed by observing peaks corresponding to $[M+H]^+$ (expected 1435.72, observed 1435.09), $[M+2H]^{2+}$ (expected 718.37, observed 718.30), and $[M+H+Na]^{2+}$ (expected 729.36, observed 729.77),



B

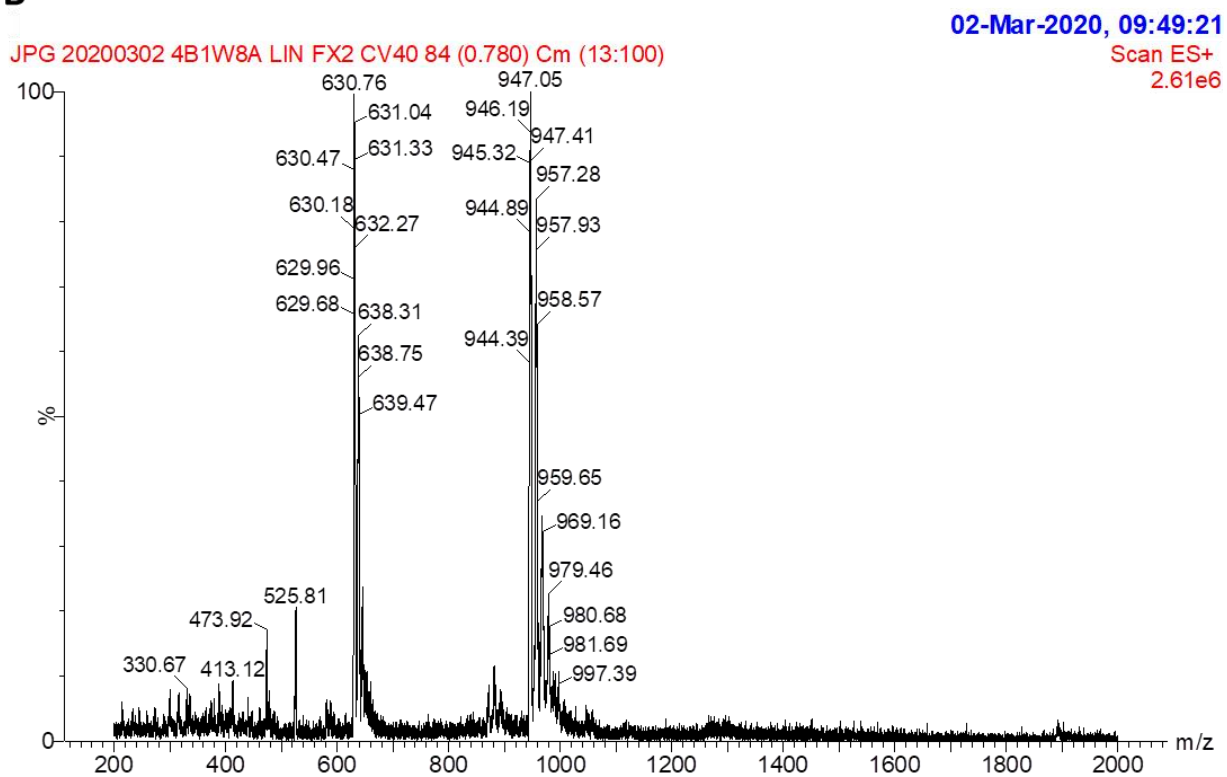


Figure S19: SUPR4B1W8A-fluorescein (Linear). **A)** Preparative HPLC purification (A_{220}) of crude product (5-95% ACN over 30 min. **B)** Electrospray ionization mass spectroscopy. The product was confirmed by observing peaks corresponding to $[M+3H]^{3+}$ (expected 631.95, observed 631.04) and $[M+2H]^{2+}$ (expected 947.43, observed 947.41)

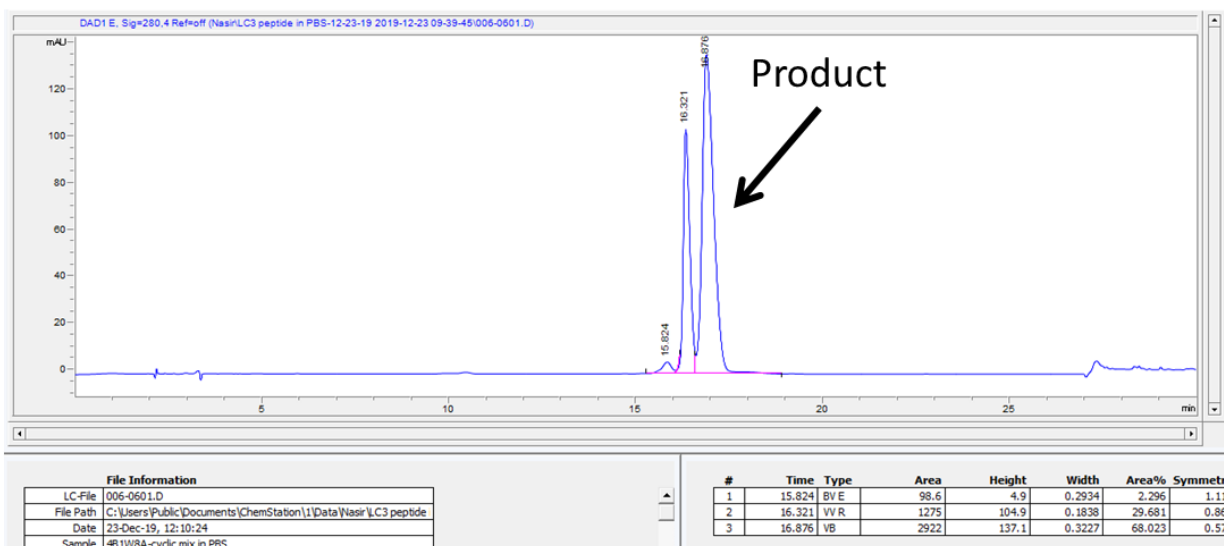
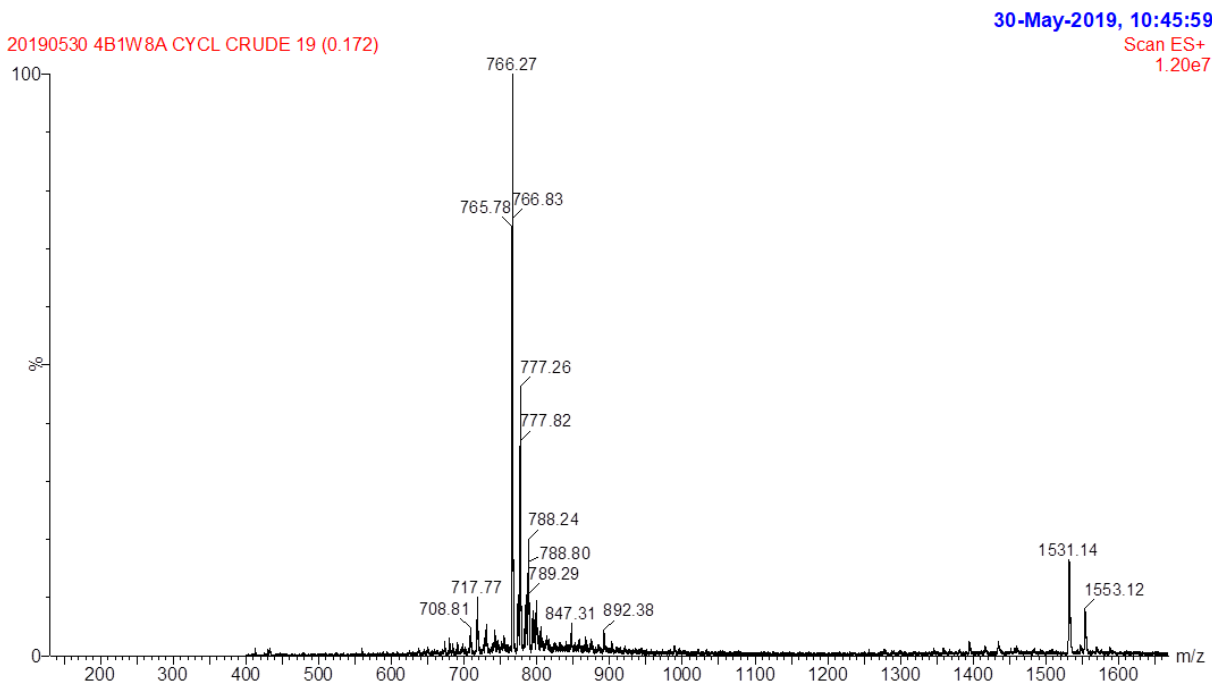
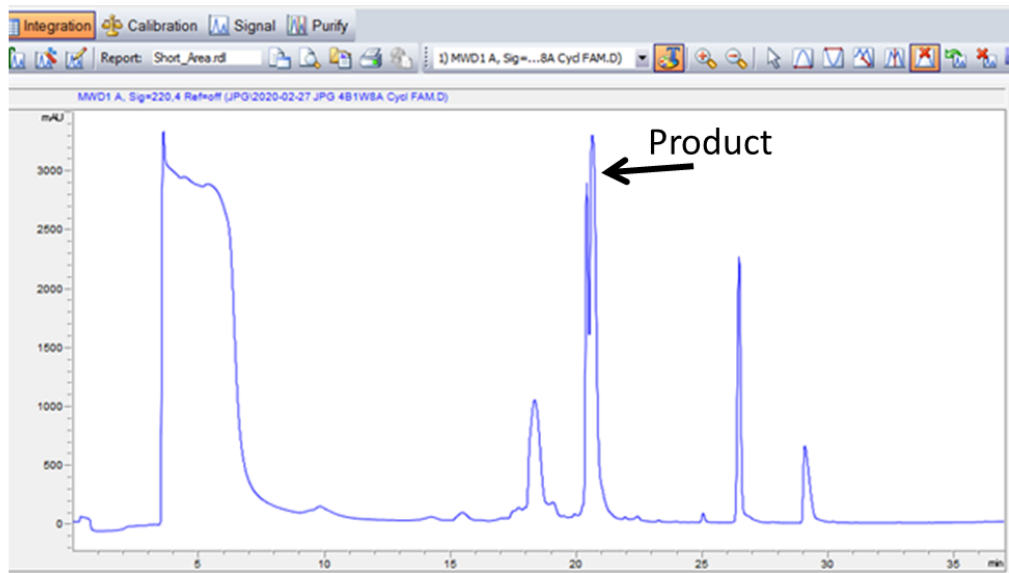
A**B**

Figure S20: SUPR4B1W8A (Cyclic). **A**) Analytical HPLC trace (A_{280}) of purified product (10-30% ACN over 30 min). **B**) Electrospray ionization mass spectrometry. The product was confirmed by observing peaks corresponding to $[M+H]^+$ (expected 1531.75, observed 1531.14.), $[M+2H]^{2+}$ (expected 766.38, observed 766.27), and $[M+H+Na]^{2+}$ (expected 777.37, observed 777.26)



B

JPG 20200302 4B1W8A CYCL FX2 CV40 20 (0.184) Cm (4:104)

02-Mar-2020, 09:37:53

Scan ES+
5.72e6

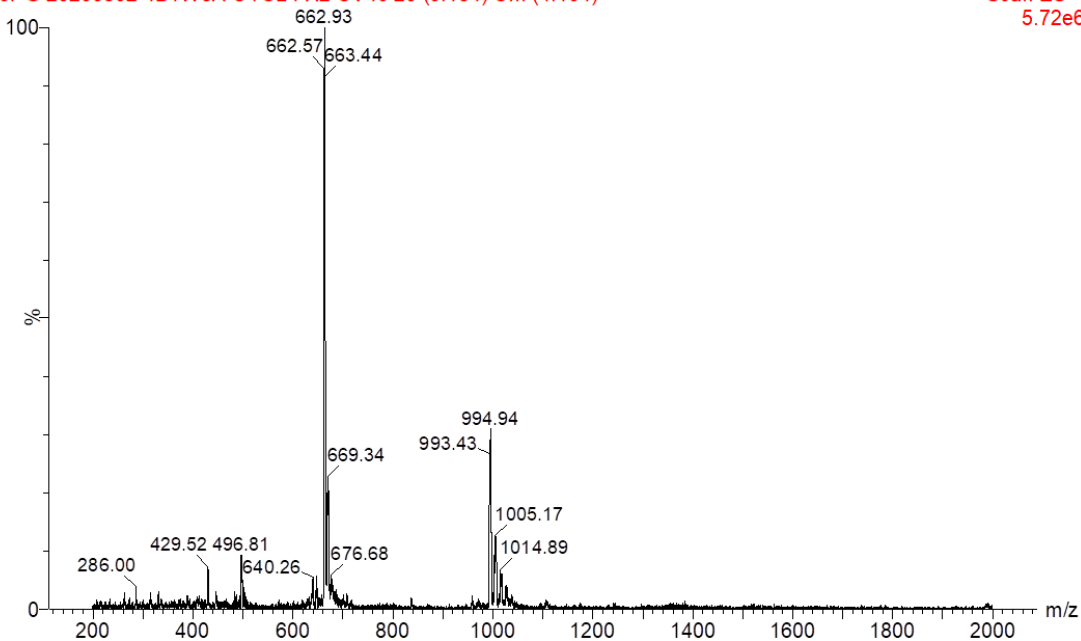


Figure S21: SUPR4B1W8A-fluorescein (Cyclic). **A)** Preparative HPLC (A_{220}) purification of crude product (5-95% ACN over 30 min). **B)** Electrospray ionization mass spectroscopy. The product was confirmed by observing peaks corresponding to $[M+3H]^{3+}$ (expected 663.96, observed 663.44) and $[M+2H]^{2+}$ (expected 995.44, observed 994.94)

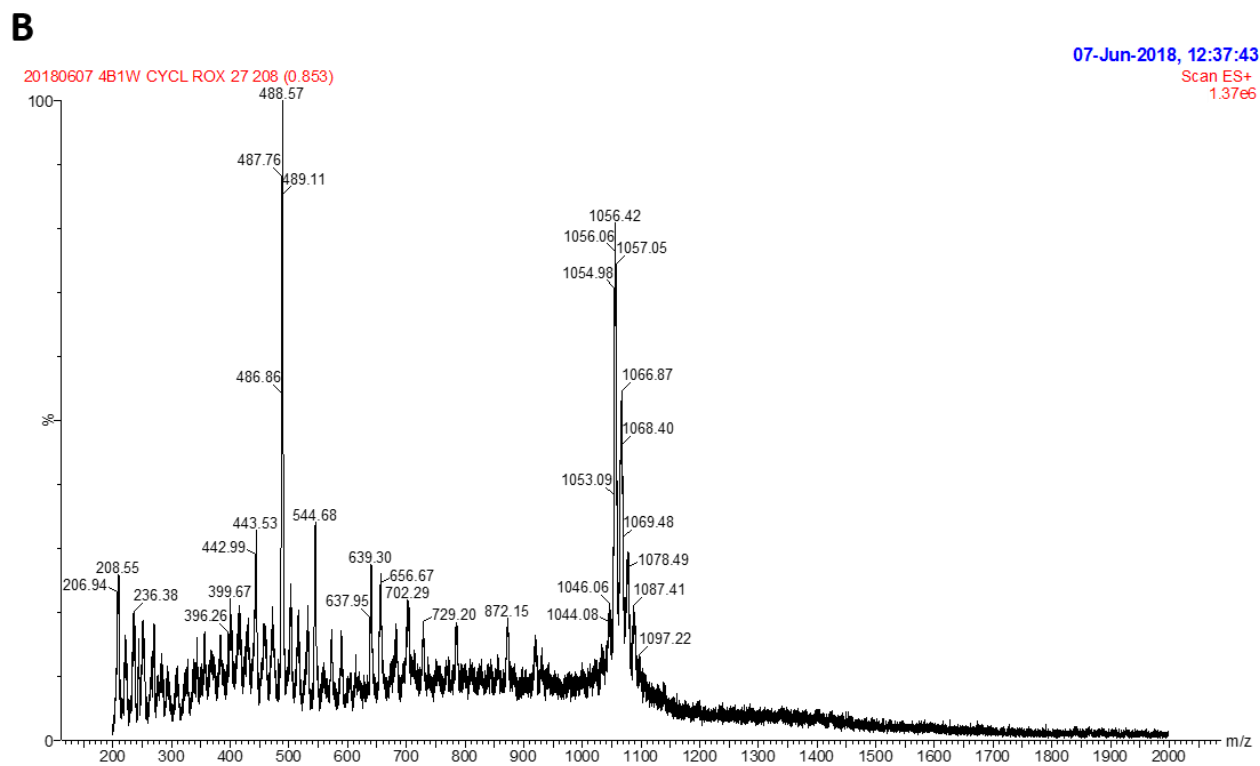
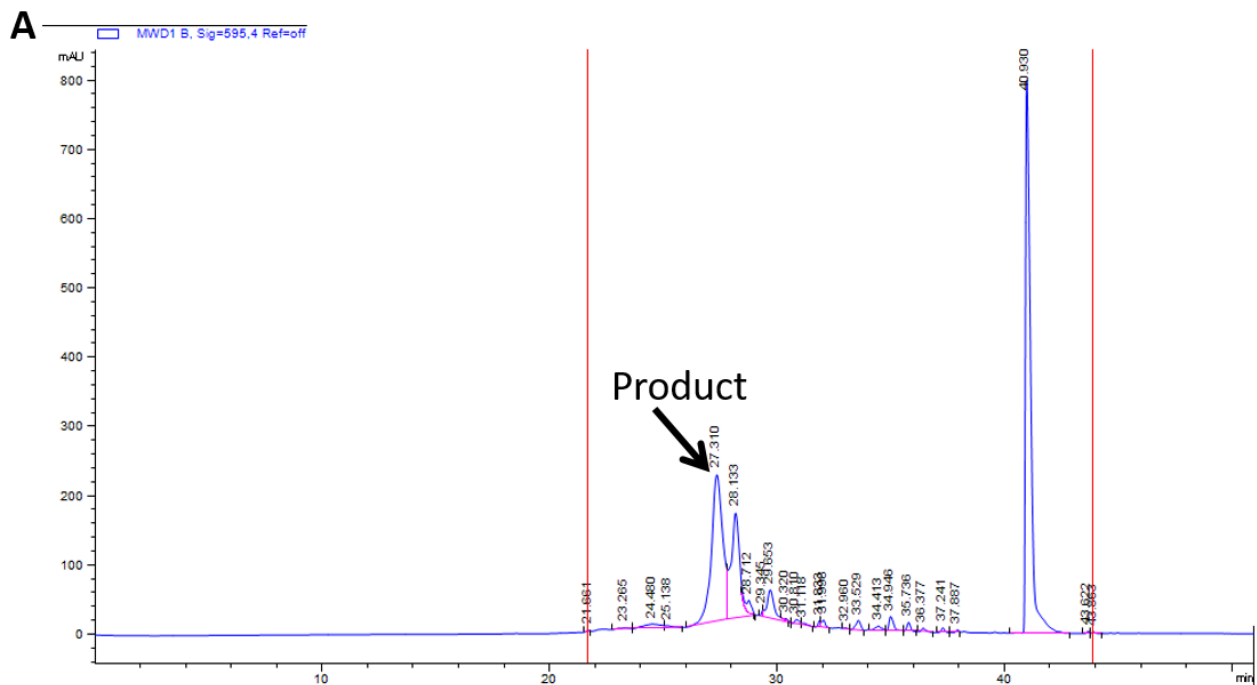


Figure S22: SUPR4B1W-ROX (cyclic). **A)** Preparative HPLC (A_{595}) purification of crude product (5-95% ACN over 45 min) **B)** Electrospray ionization mass spectrometry. The product was confirmed by observing peaks corresponding to $[M+2H]^{2+}$ (expected 1056.03, observed 1056.42) and $[M+H+Na]^{2+}$ (expected 1067.02, observed 1066.87)

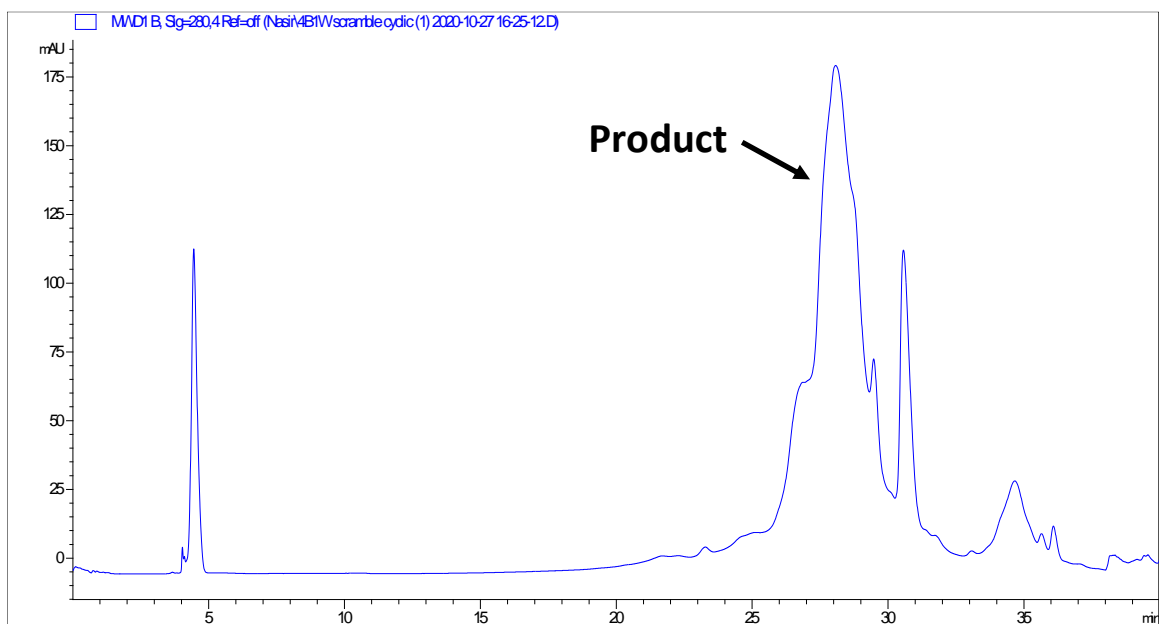
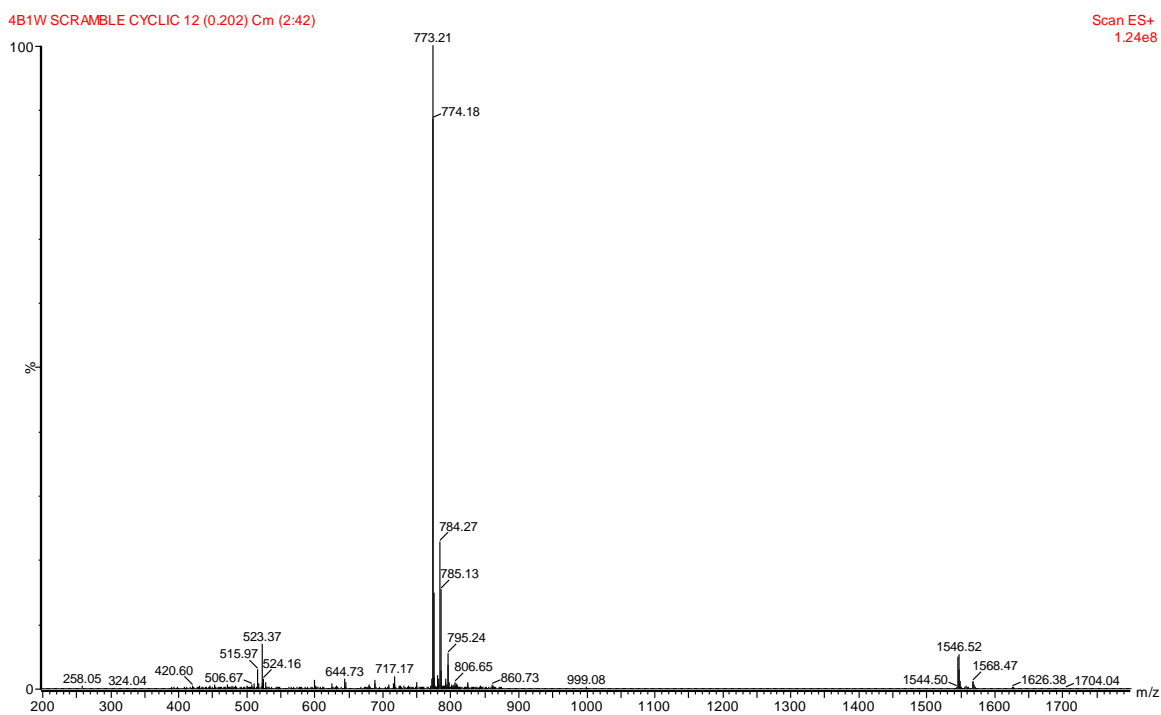
A**B**

Figure S23: SUPR4B1W scrambled (cycVWHAZRTMPKSG-Pra). **A)** Preparative HPLC (A_{280}) purification of crude product (10-30% ACN over 35 min). **B)** Electrospray ionization mass spectrometry. The product was confirmed by observing peaks corresponding to $[M+3H]^{3+}$ (expected 515.93, observed 515.97), $[M+2H+Na]^{3+}$ (expected 523.25, observed 523.37), $[M+2H]^{2+}$ (expected 773.39, observed 773.21), $[M+H+Na]^{2+}$ (expected 784.39, observed 784.27) and $[M+H]^{+}$ (expected 1545.77, observed 1546.52).

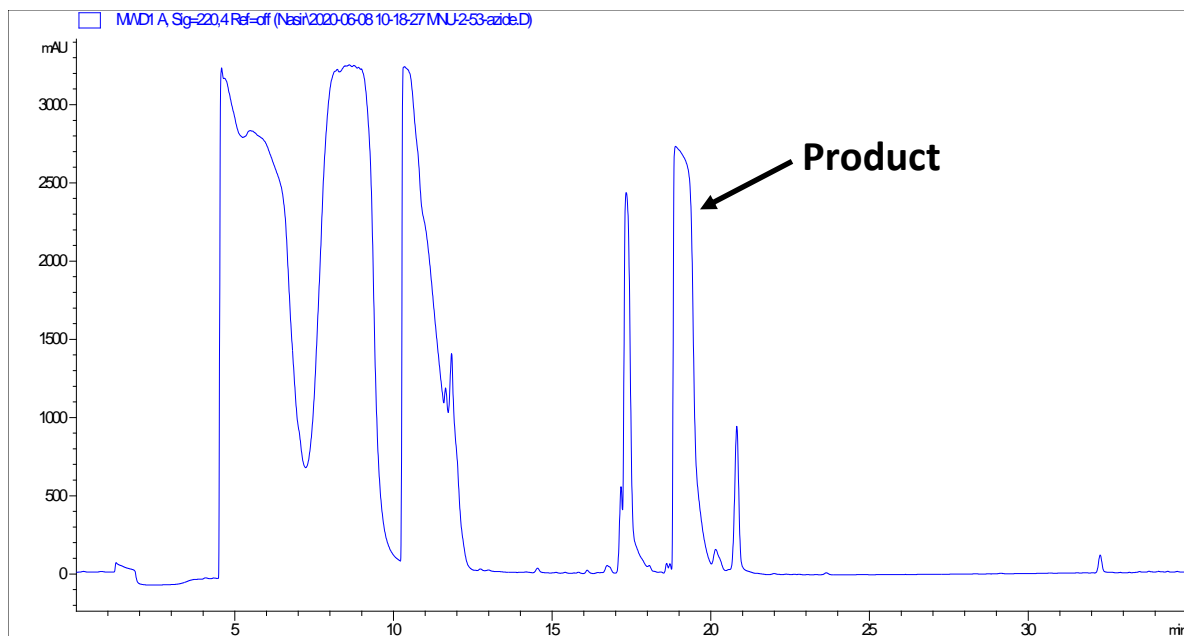
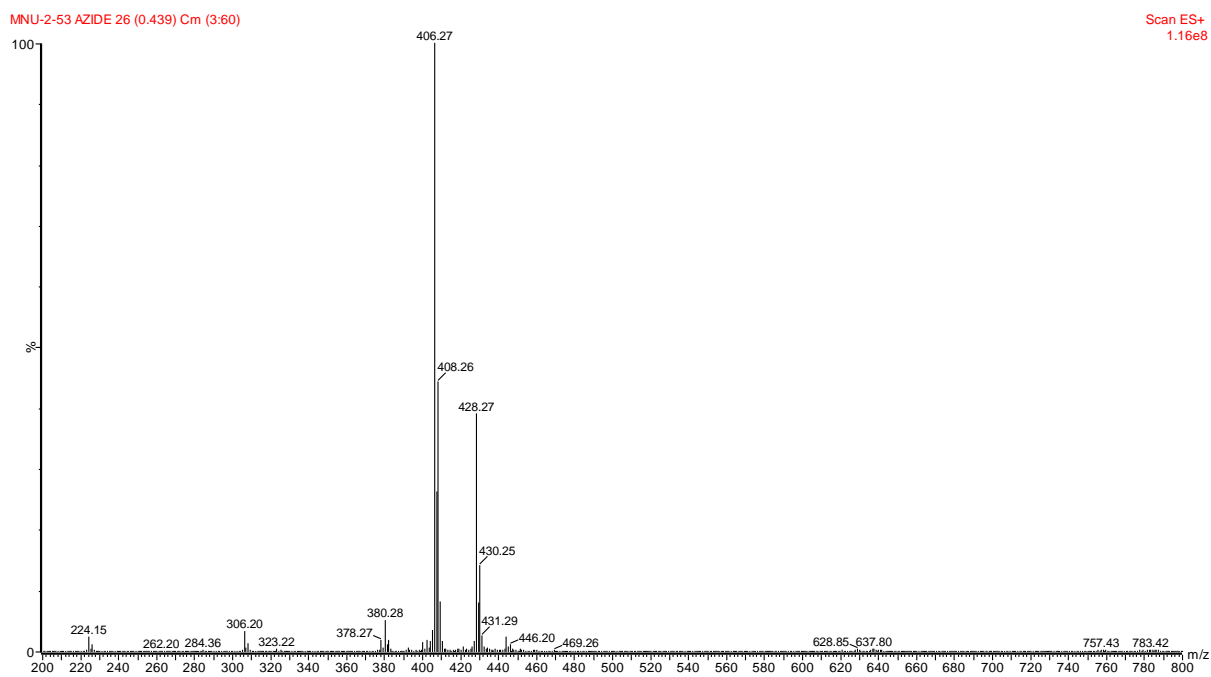
A**B**

Figure S24: Chloroalkane azide. **A)** Preparative HPLC (A₂₂₀) purification of crude product (10-95% ACN over 35 min). **B)** Electrospray ionization mass spectrometry. The product was confirmed by observing peaks corresponding to [M+H]⁺ (expected 406.22, observed 406.27) and [M+Na]⁺ (expected 528.20, observed 528.27).

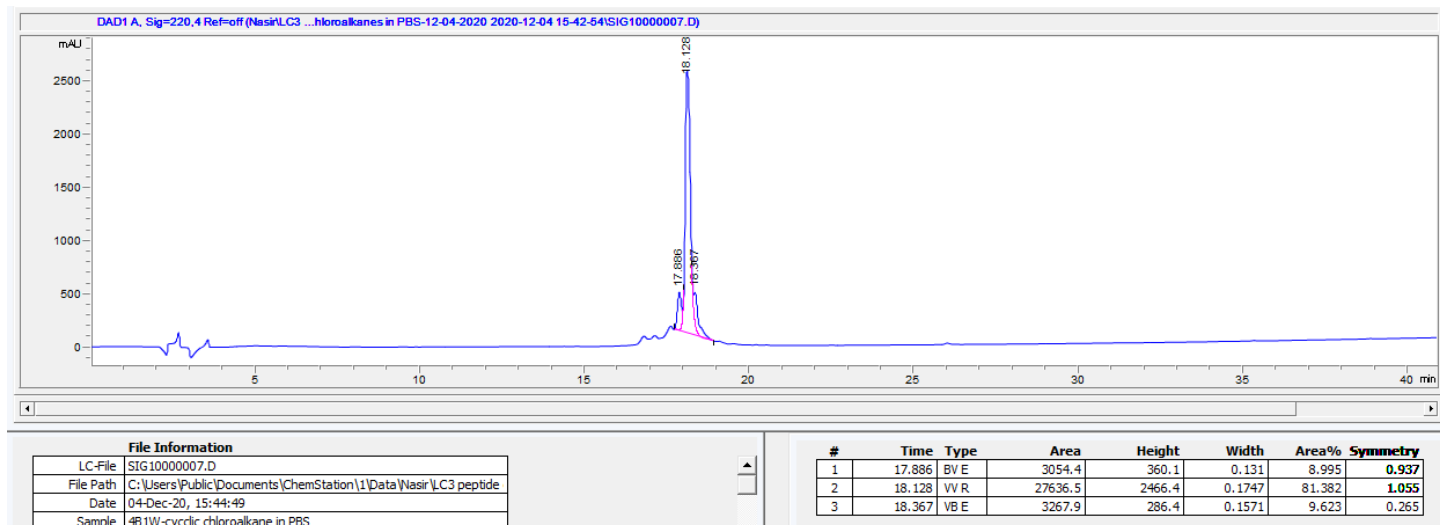
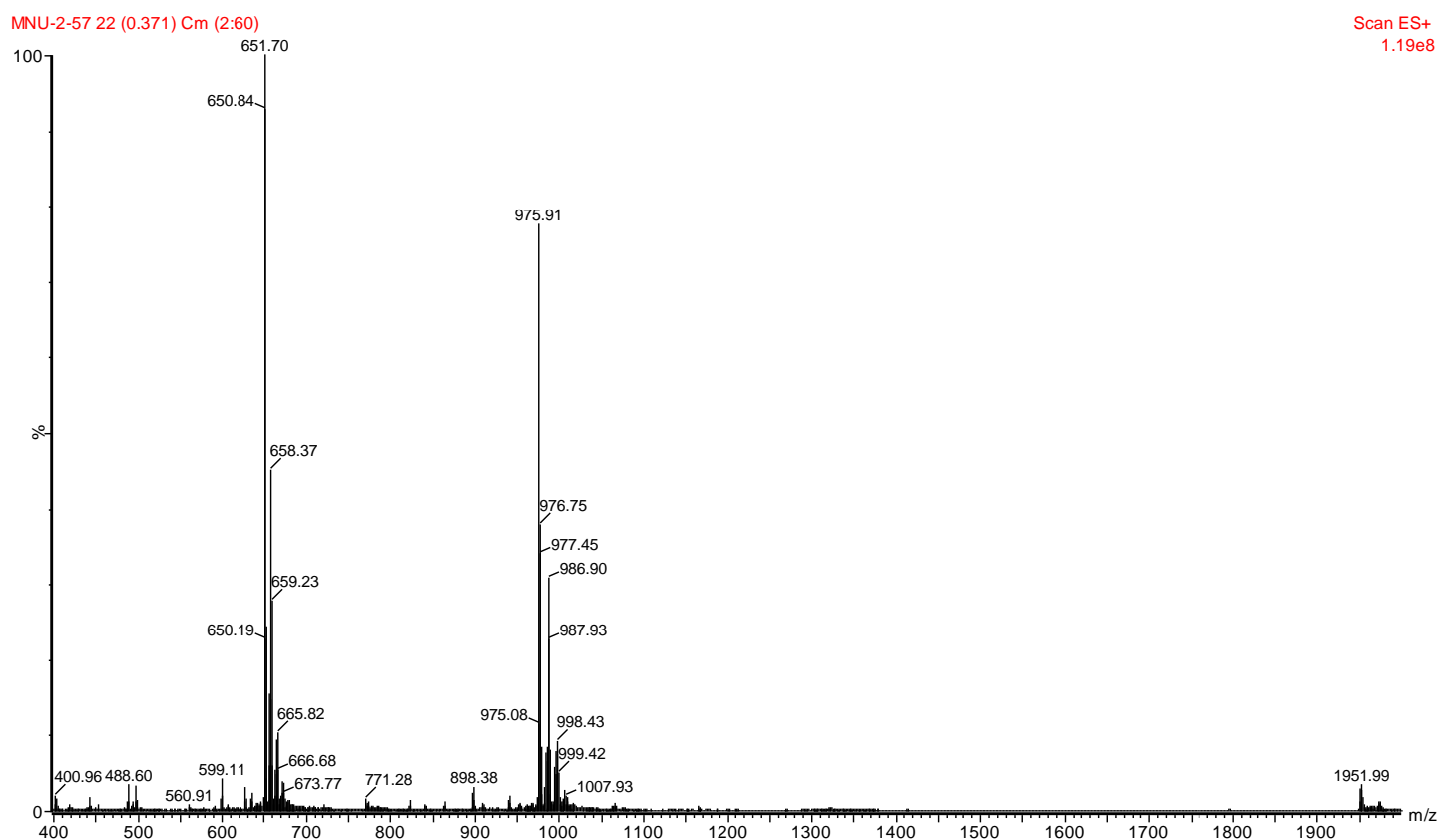
A**B**

Figure S25: SUPR4B1W cyclic chloroalkane **A)** Analytical HPLC trace (A_{220}) of purified product (10-95% ACN over 40 min). **B)** Electrospray ionization mass spectroscopy. The product was confirmed by observing peaks corresponding to $[M+3H]^{3+}$ (expected 650.99, observed 651.70), $[M+2H+Na]^{3+}$ (expected 658.32, observed 658.37), $[M+2H]^{2+}$ (expected 975.99, observed 975.91), $[M+H+Na]^{2+}$ (expected 986.98, observed 986.90) and $[M+H]^+$ (expected 1950.98, observed 1951.99).

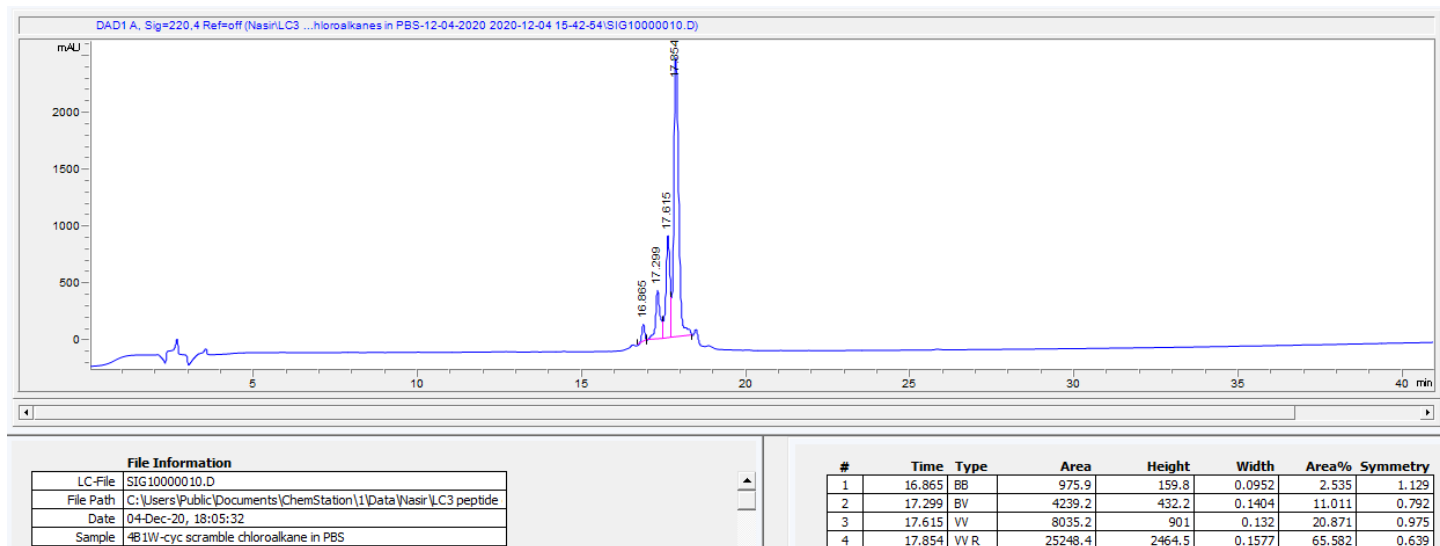
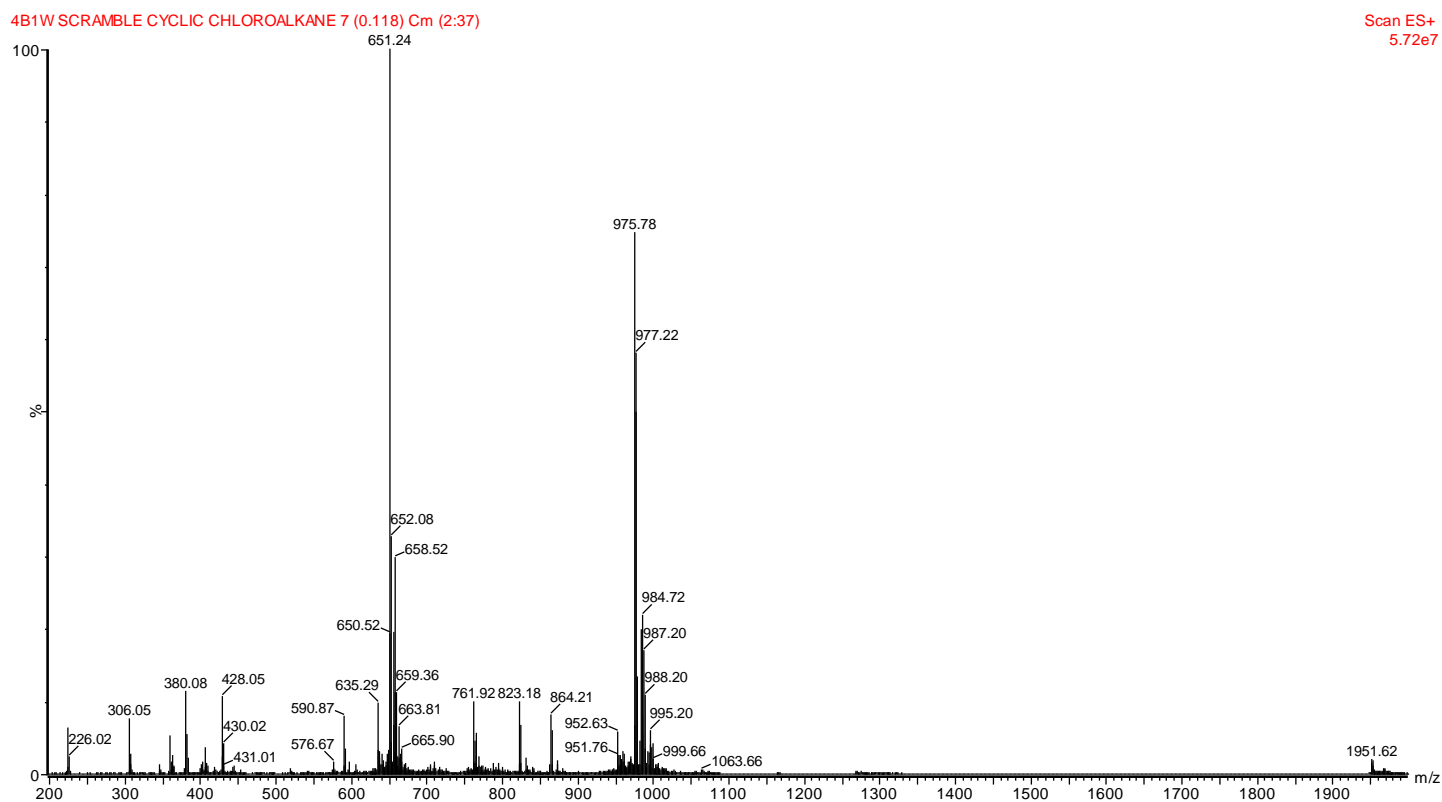
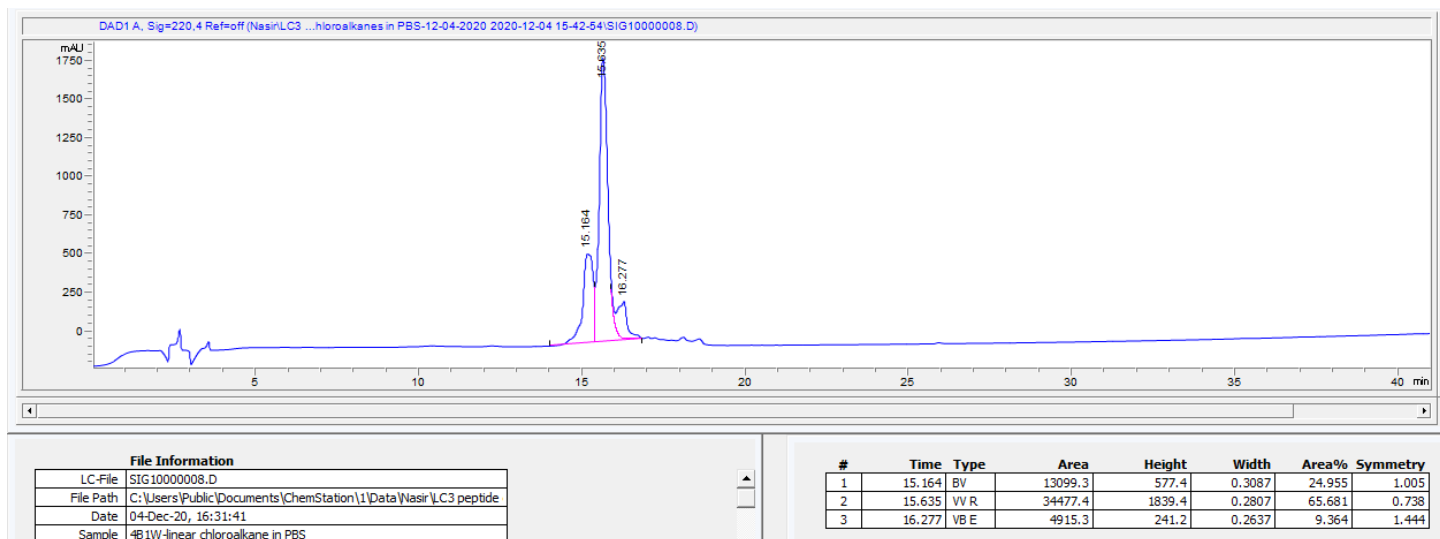
A**B**

Figure S26: SUPR4B1W cyclic (scrambled) chloroalkane **A)** Analytical HPLC trace (A_{220}) of purified product (10-95% ACN over 40 min). **B)** Electrospray ionization mass spectroscopy. The product was confirmed by observing peaks corresponding to $[M+3H]^{3+}$ (expected 650.99, observed 651.24), $[M+2H+Na]^{3+}$ (expected 658.32, observed 658.52), $[M+2H]^{2+}$ (expected 975.99, observed 975.78) and $[M+H]^+$ (expected 1950.98, observed 1951.62).

A**B**

MNU-2-67 56 (0.945) Cm (2:59)

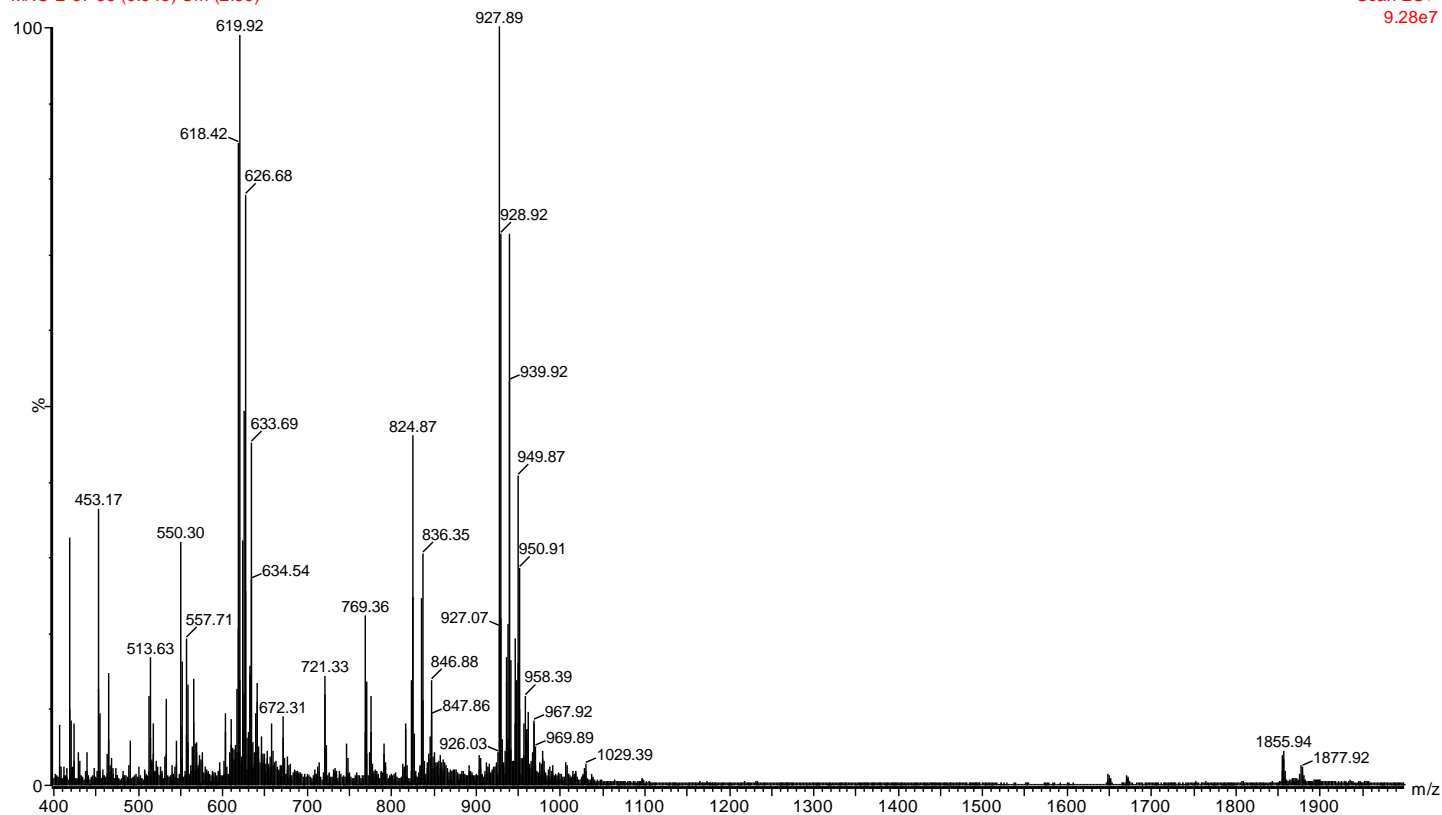
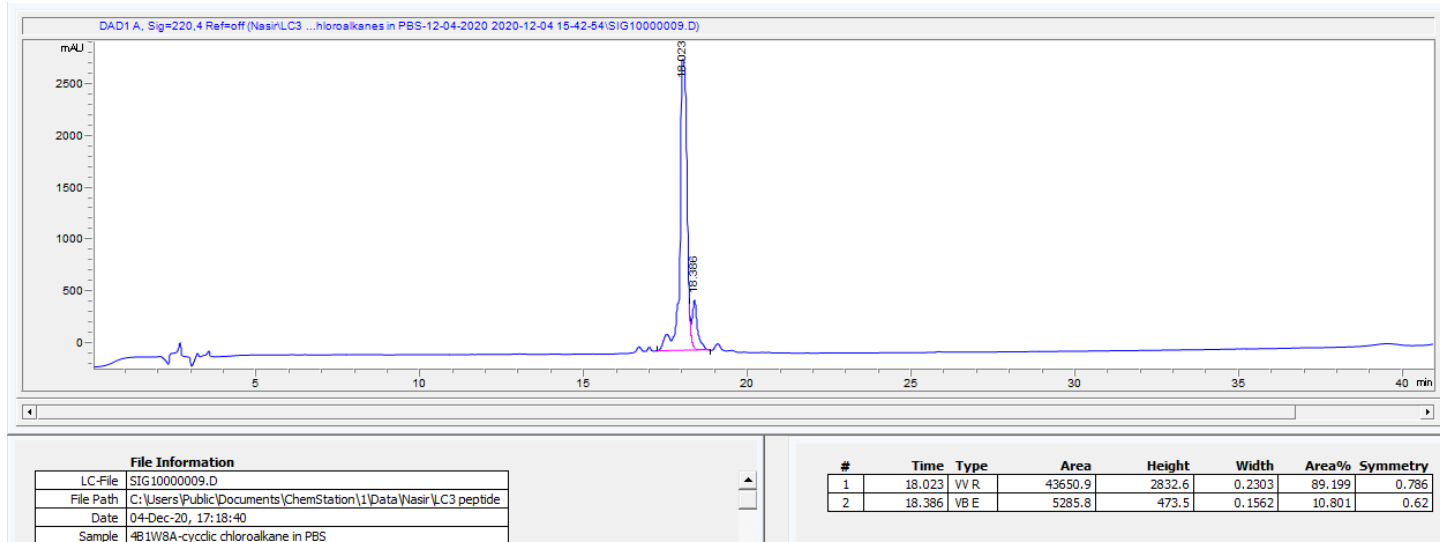
Scan ES+
9.28e7

Figure S27: SUPR4B1W linear chloroalkane A) Analytical HPLC trace (A_{220}) of purified product (10-95% ACN over 40 min). **B)** Electrospray ionization mass spectroscopy. The product was confirmed by observing peaks corresponding to $[M+3H]^{3+}$ (expected 618.99, observed 618.42), $[M+2H+Na]^{3+}$ (expected 633.75, observed 533.69), $[M+2H]^{2+}$ (expected 927.98, observed 927.89) and $[M+H]^+$ (expected 1854.96, observed 1855.94).

A**B**

MNU-2-69.7 (0.118) Cm (2:29)

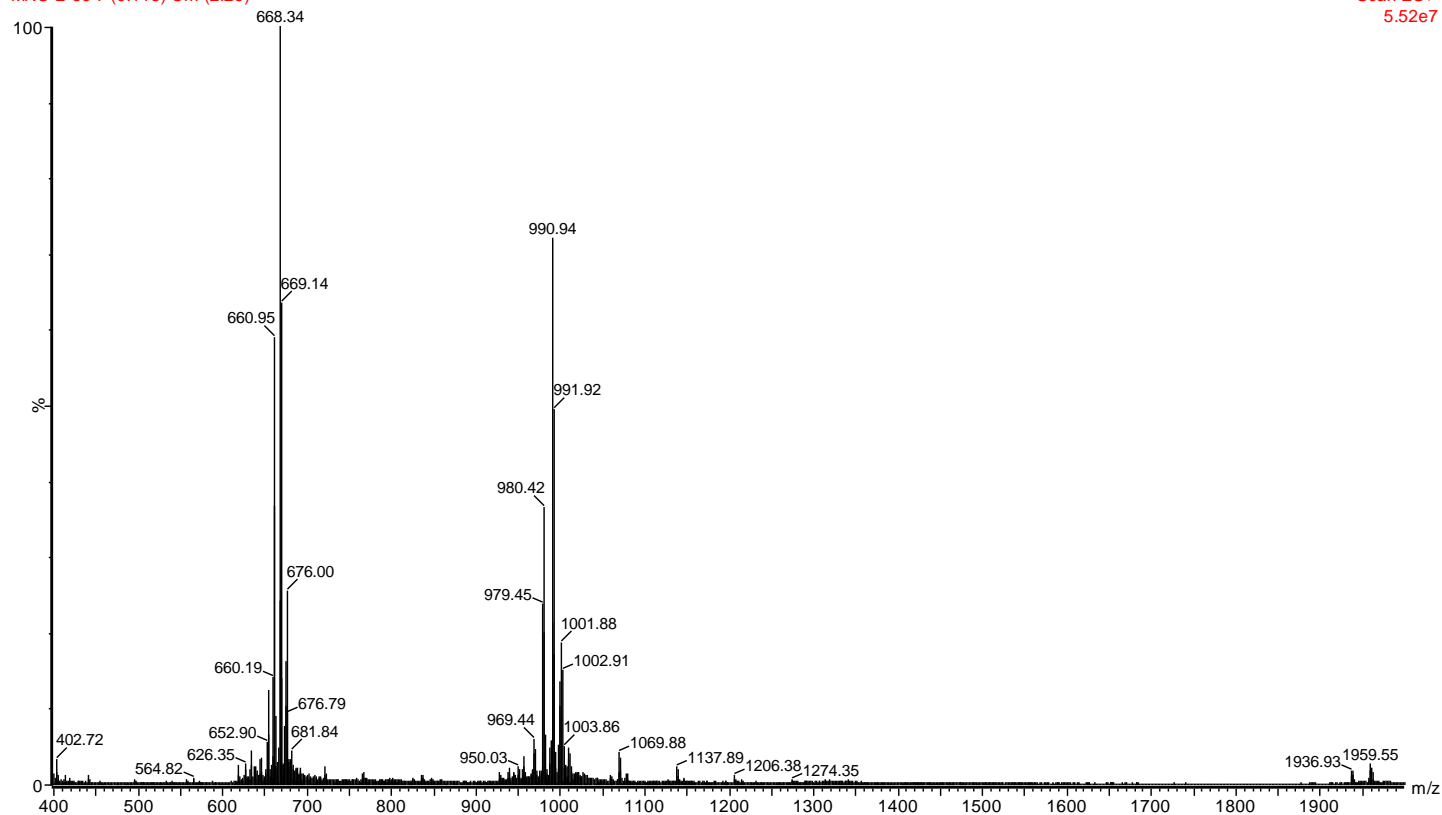
Scan ES+
5.52e7

Figure S28: SUPR4B1W8A cyclic chloroalkane **A)** Analytical HPLC trace (A_{220}) of purified product (10-95% ACN over 40 min). **B)** Electrospray ionization mass spectroscopy. The product was confirmed by observing peaks corresponding to $[M+H+2Na]^{3+}$ (expected 661.08, observed 660.95), $[M+3Na]^{3+}$ (expected 668.31, observed 668.34), $[M+H+Na]^{2+}$ (expected 979.97, observed 980.42), $[M+2Na]^{2+}$ (expected 990.96, observed 990.94) and $[M+H]^+$ (expected 1936.96, observed 1936.93).

Supplemental Bibliography

1. Lamark T, Perander M, Outzen H, et al. Interaction Codes within the Family of Mammalian Phox and Bem1p Domain-containing Proteins. *J Biol Chem*. 2003;278(36):34568-34581. doi:10.1074/jbc.M303221200
2. Pankiv S, Clausen TH, Lamark T, et al. p62/SQSTM1 binds directly to Atg8/LC3 to facilitate degradation of ubiquitinated protein aggregates by autophagy*[S]. *J Biol Chem*. 2007;282(33):24131-24145. doi:10.1074/jbc.M702824200
3. Fiacco S V., Kelderhouse LE, Hardy A, et al. Directed Evolution of Scanning Unnatural-Protease-Resistant (SUPR) Peptides for in Vivo Applications. *ChemBioChem*. 2016:1643-1651. doi:10.1002/cbic.201600253
4. Bolte S, Cordelières FP. A guided tour into subcellular colocalization analysis in light microscopy. *J Microsc*. 2006. doi:10.1111/j.1365-2818.2006.01706.x
5. Peraro L, Deprey KL, Moser MK, Zou Z, Ball HL, Levine B, Kritzer JA. Cell Penetration Profiling Using the Chloroalkane Penetration Assay. *J. Am. Chem. Soc.* 2018. doi.org/10.1021/jacs.8b06144